

Electronic Supporting Information

**Cobalt Catalysts (Co-N-C) for C-O Bond Cleavage in Lignin-Derived Aryl Ethers and Lignin**

Daniel Bautista-García,<sup>a</sup> David Macias-José,<sup>a</sup> Paola Aguillón-Rodríguez,<sup>a</sup> Obed Pérez-Reyes<sup>b</sup> and Carmen Ortiz-Cervantes,<sup>\*a</sup>

<sup>a</sup> Instituto de Química, Universidad Nacional Autónoma de México, CU, Coyoacán, 04510, Ciudad de México, México.

<sup>b</sup> Instituto Politécnico Nacional, Centro de Investigación en Ciencia Aplicada y Tecnología Avanzada, Unidad Legaria, Ciudad México, México.

carmen.ortiz@iquimica.unam.mx

*Table of Contents*

1. Characterization methods	S2
2. Characterization of Co-1	S4
3. Synthesis of substrates	S15
3.1. Synthesis of MM-3	S15
3.2. Synthesis of MM-2	S16
3.3. Synthesis of MM-1	S16
4. Synthesis of Co/C catalyst	S16
5. Catalytic hydrogenolysis	S17
6. Spectra and chromatograms	S18
7. References	S35

## 1. Characterization Methods

For cobalt materials as well as for organic compounds, various identification and characterization techniques were used, sample preparation was performed according to each specific protocol described below.

### Nuclear Magnetic Resonance (NMR) Studies

$^1\text{H}$ ,  $^{13}\text{C}\{^1\text{H}\}$  and HSQC NMR spectra were recorded at room temperature on a 400 MHz Bruker Avance III spectrometer in  $\text{CDCl}_3$ , unless otherwise stated.  $^1\text{H}$  and  $^{13}\text{C}\{^1\text{H}\}$  chemical shifts ( $\delta$ , ppm) are reported relative to the residual proton resonance in the corresponding deuterated solvent.

### Mass Spectrometry

A Jeol mass spectrometer SX 102 A was used with the direct analysis in real time (DART).

### GC-MS

Conversion and selectivity of catalytic reactions were determined via GC-MS analysis performed on Agilent 5975C system equipped with a 30 m DB-5MS capillary (0.32 mm ID) column), He 99.999%.

### Electron Paramagnetic Resonance (EPR)

Solid samples were placed in quartz tubes of 1.34 cm diameter and 0.15 cm thickness. Loaded tubes were then introduced in a Jeol JES-TE300 spectrometer operating at X band frequency (9.4 GHz) at 100 kHz field modulation, with a cylindrical cavity (TE011 mode). Samples were run at 77 K.

### Fourier Transform Infrared (FTIR) spectra

The ATR-IR spectra were determined on a FTIR/FIR spectrum FT-IR NICOLET IS-50, Thermo Fisher Scientific, measuring 32 scans per sample, from 4000 to 400  $\text{cm}^{-1}$  with a resolution of 2  $\text{cm}^{-1}$ , the sample did not require previous preparation.

### Powder X-ray Diffraction (PXRD)

Powder X-Ray diffraction measurements were performed on a Rigaku Ultima IV diffractometer with  $\text{Cu K}\alpha$  radiation ( $\lambda=1.54056$  Å) at 40 kV and 44 mA. The instrument was operating in a Bragg Brentano geometry with a step increment of  $0.02^\circ$  and an acquisition time of one second per step.

### Transmission Electron Microscopy

Transmission electron microscopy studies were carried out in a Jeol ARM-200F operated at 200 kV using copper grids (mesh size of 300 covered with a lacey carbon film) equipped with on a holey carbon. The samples were dispersed in anhydrous toluene.

## **X-ray photoelectron spectroscopy (XPS)**

XPS spectra were recorded at room temperature using a K-alpha+ spectrometer Thermo Fisher Scientific Co. Equipped with an Al Ka (1486.6 eV) monochromatic X-ray source, a dual-beam flood gun for charge neutralization, and 180 double focusing hemispherical analyzer operating in a constant analyzer energy mode (CAE). The measurement spot size was 400  $\mu\text{m}$  and a base pressure of  $1 \times 10^{-9}$  mbar was held in the analytical chamber. Survey scans were recorded using 400  $\mu\text{m}$  spot size and fixed pass energy of 200 eV, whereas high resolution spectra were recorded at 20 eV of pass energy with a step size of 0.1 eV. Charge corrections for all the spectra were referenced to the position of the C1s adventitious peak at 284.8 eV. All spectra were processed with the Avantage software (v5.9925) provided by Thermo-Fisher Scientific Co. The curve fitting was performed with a Voigt function and a Shirley-type background. Transition metals having unpaired electrons in the *d* orbitals, such as Co(II), exhibit the so-called multiplet splitting feature in their XPS spectra, which is manifested as the appearance of additional peaks as a consequence of the different final states due to the coupling of the unpaired spins in *d* orbitals with the unpaired spin in the nucleus produced by the photoemission of an electron, in this case from the Co2p level. In addition, there can be present shake-up and plasmon loss structures which also contribute to the final spectrum shape. In a transition metal spectrum with the mentioned features the number of contributions as well as their positions and intensities can be different even for the same atom in the same oxidation state since these structures are very sensitive to the chemical environment, as previously described by Biesinger et al <sup>1</sup> and Yang et al<sup>2</sup> who developed multiplet structure models of transition metal oxides and hydroxides and the contributions do not necessarily have a single chemical identity but contribute to reproduce the spectral shape of the analyzed species and thus can be used in subsequent curve fitting procedures.<sup>3</sup>

## **Inductively coupled plasma spectroscopy (ICP-MS) analysis**

ICP-MS analysis for Co materials was measured using Thermo Scientific Element XR High-Resolution ICP-MS after digesting materials in aqua regia.

## **Elemental Analysis**

Elemental analysis of **Co/C** and **Co-1** was carried out in Thermo Scientific/Flash 2000.

## **Gel permeation chromatography/Size exclusion chromatography**

The GPC/HPSEC analysis were carry out UV/Vis detector equipped the molecular weights and the molecular distributions (MWD) of the samples from lignin hydrogenolysis product were determinate by GPC chromatograph in Water Alliance e2695 chromatograph separation module apparatus equipped with detector multi angle light scattering (MALLS) Wyatt Technology, model DAWN EOS, polystyrene was used to calibration. The samples were dissolved in THF.

## 2. Characterization of Co-1.

PDRX

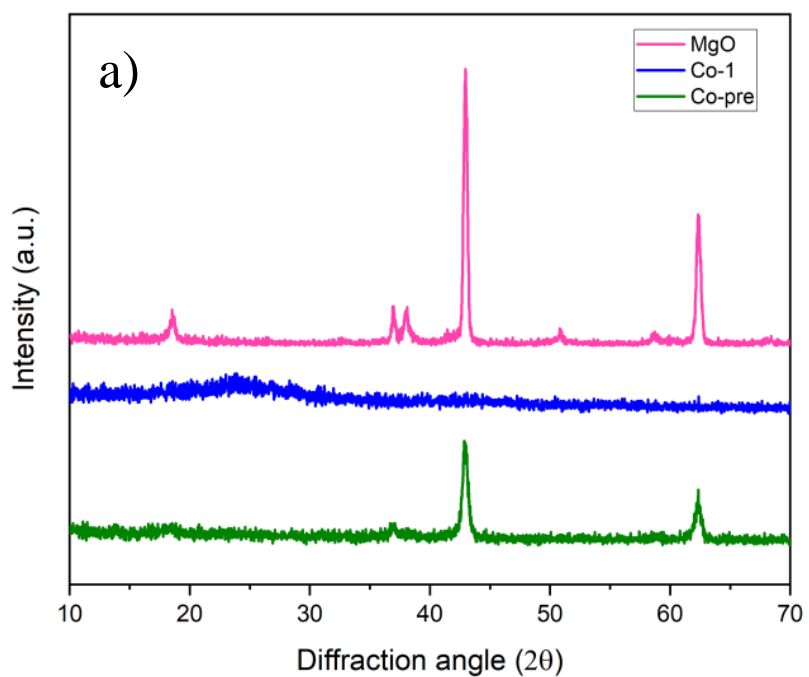


Figure S1. Powder X-ray diffraction (PDRX) patterns of Co-1 before thermal treatment, Co-1 and MgO.

XPS

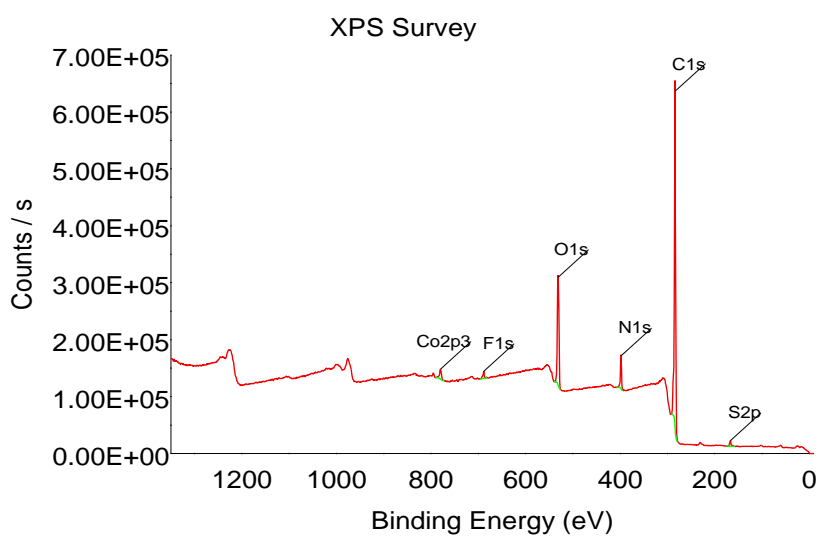


Figure S2. XPS survey spectra of the Co-1.

## Elemental Analysis and ICP

Table S1. wt% Co and N content.

Sample	Co (mg/Kg)/%wt. <sup>a</sup>	N (%) <sup>b</sup>	Co(atomic %)/%wt. <sup>c</sup>
Co-1	6040.07/0.60	5.90	0.44/1.98
Co/C	37954.63/3.79	2.91	-
Co-2	13331.42/1.32	-	-

<sup>a</sup> Obtained by IPC-MS, <sup>b</sup> elemental analysis, and <sup>c</sup> XPS.

## Elemental Analysis

No. de registro	Clave de la muestra	Valor	N [%]	C [%]	H [%]	S [%]	Fecha de análisis
225	Co-C	Teórico	2.91	90.98	1.59	---	24-08-2022
		Exp	1.29	71.33	1.25	---	

No. de registro	Clave de la muestra	Valor	N [%]	C [%]	H [%]	S [%]	Fecha de análisis
224	DM-1-DM-2	Teórico	5.90	74.19	1.15	---	24-08-2022
		Exp	9.14	59.28	3.21	---	

## TEM

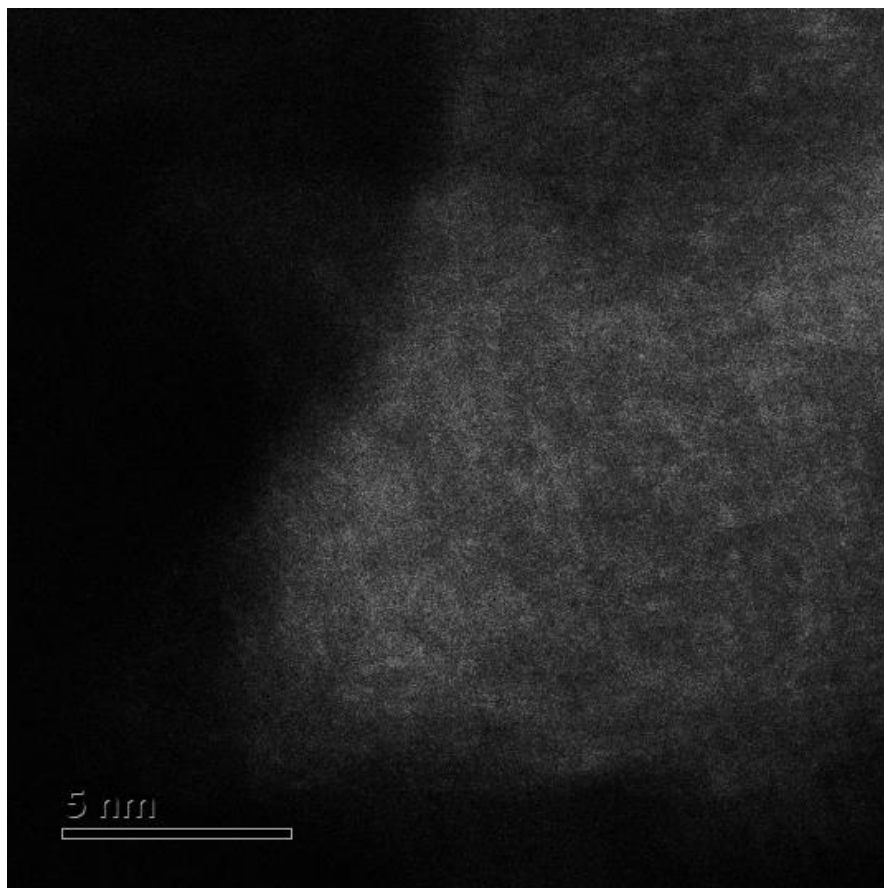
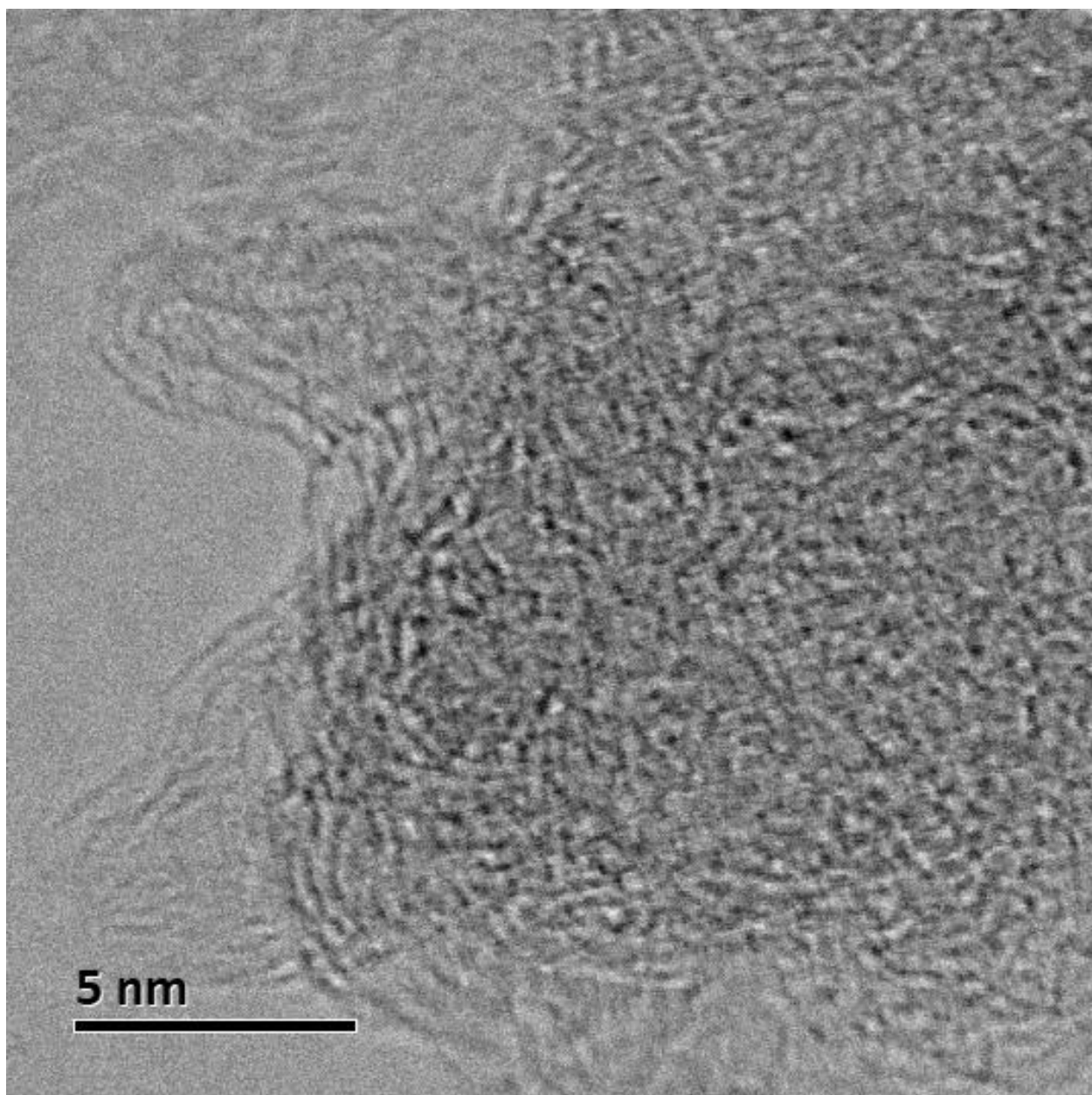
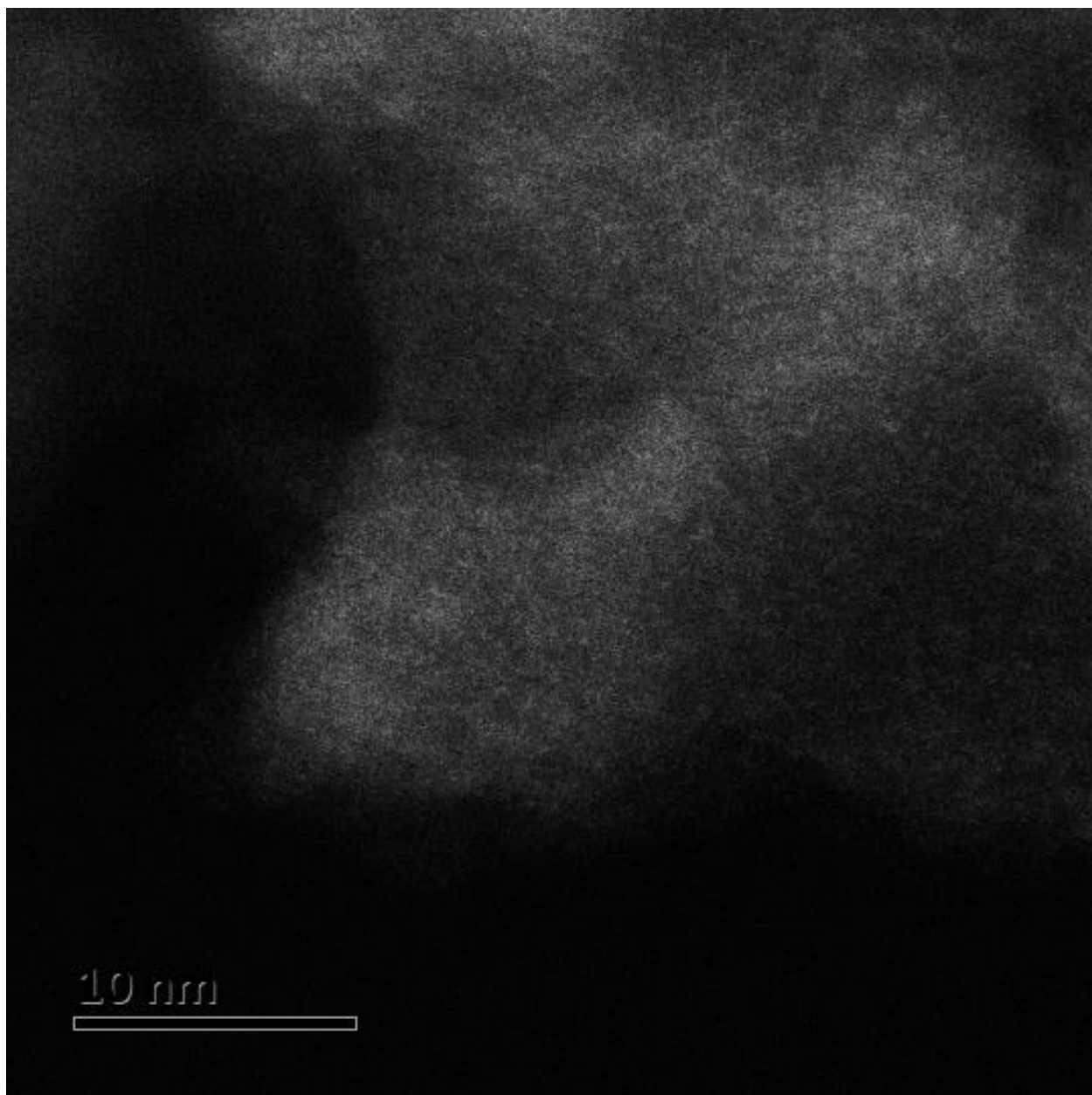


Figure S3. TEM images from Co-1 (scale = 5 nm).



**Figure S4.** TEM images from Co-1 (scale = 5 nm).



**Figure S5.** TEM images from **Co-1** (scale = 10 nm).

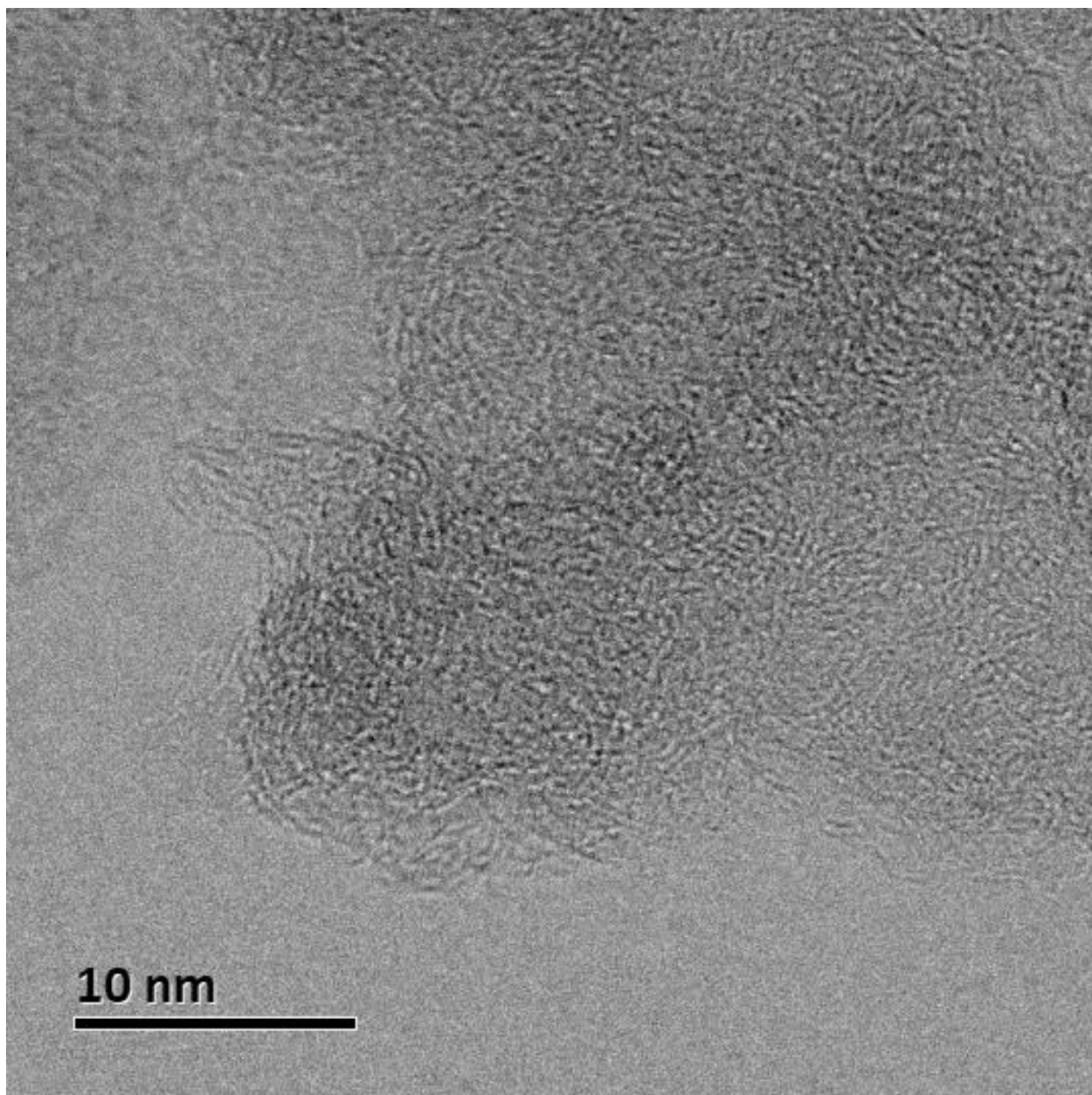


**Figure S6.** TEM images from Co-1 (scale = 10 nm).



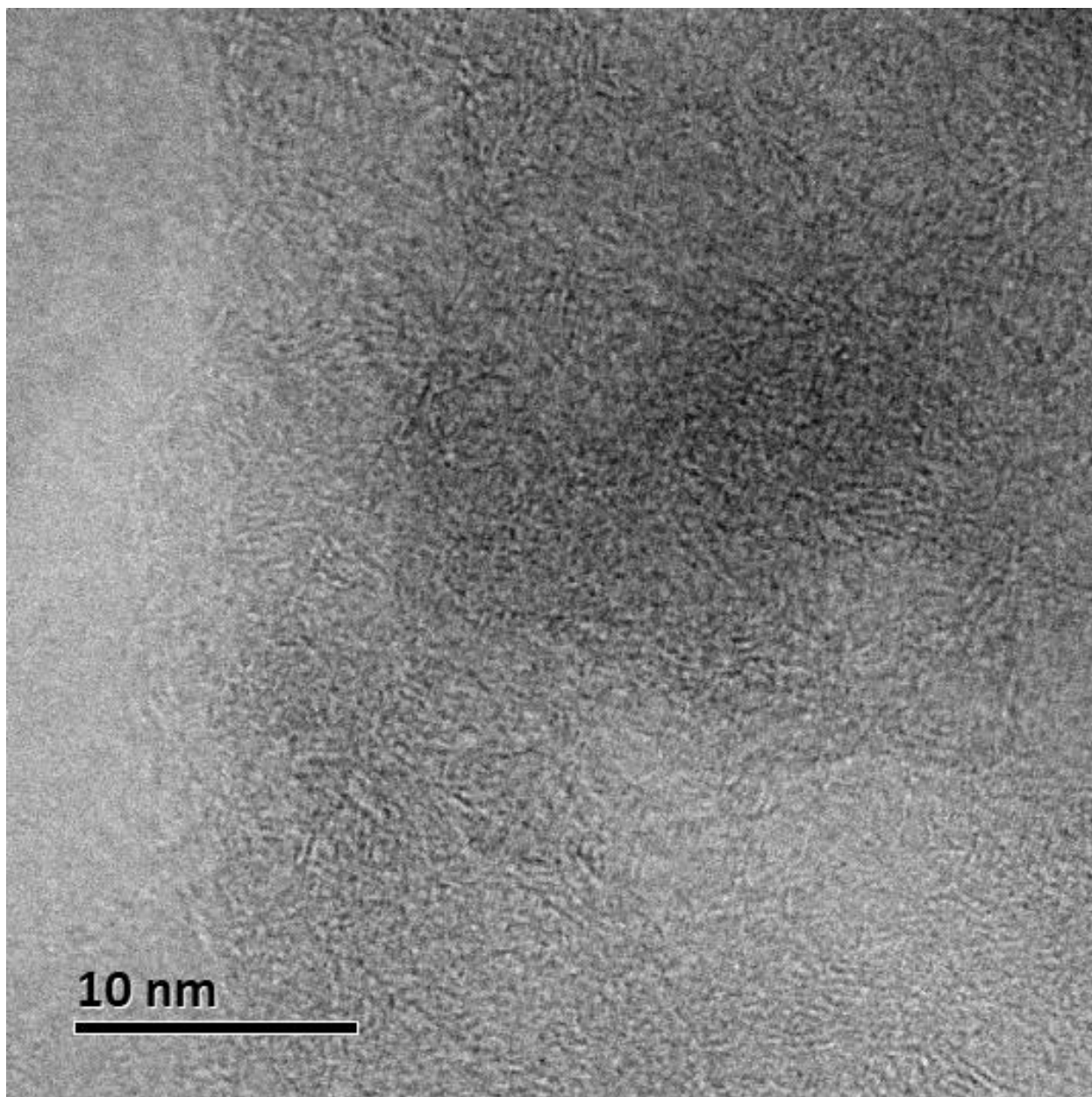


**Figure S7.** TEM images from Co-1 (scale = 10 nm).

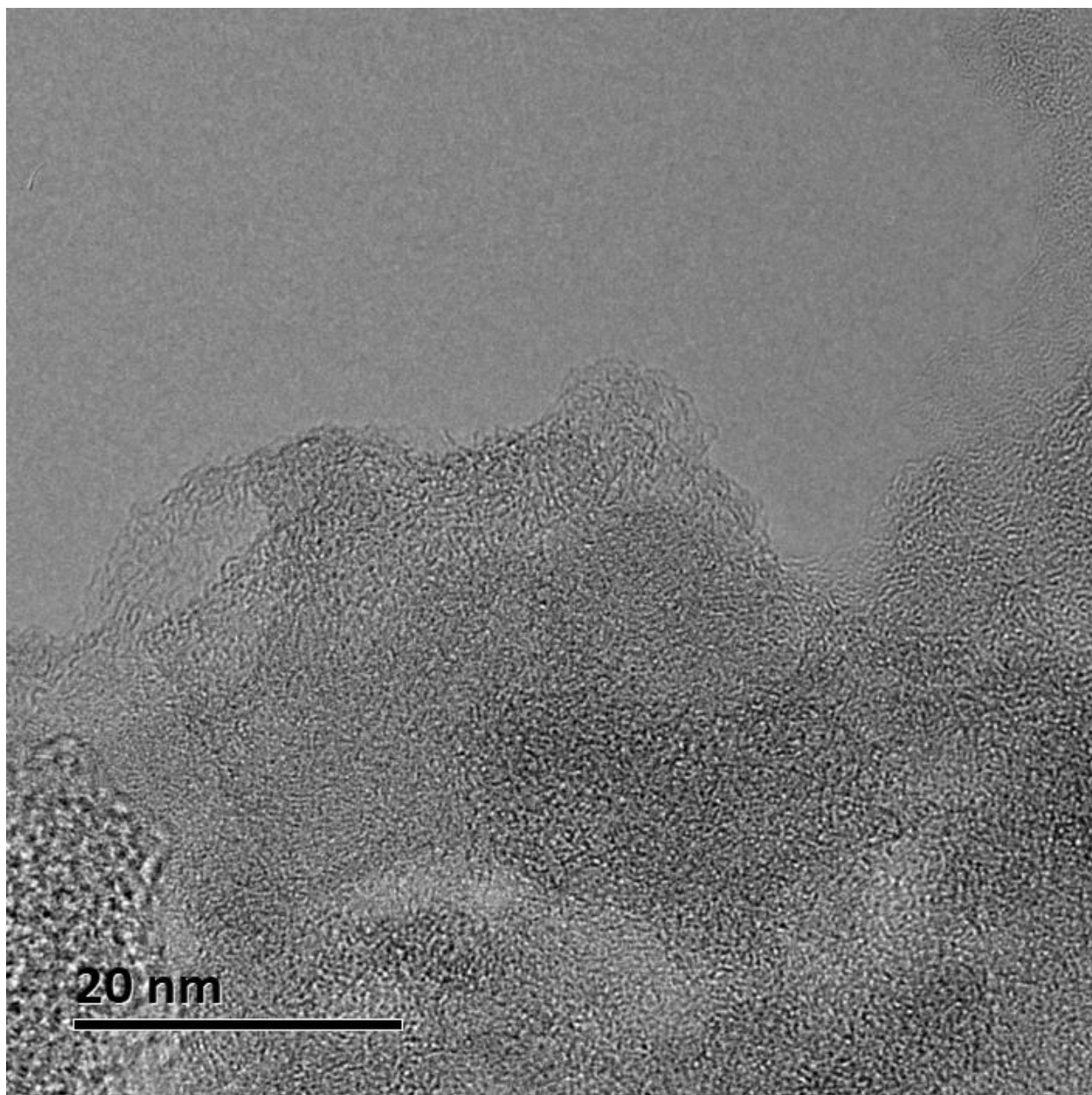


**Figure S8.** TEM images from Co-1 (scale = 20 nm).

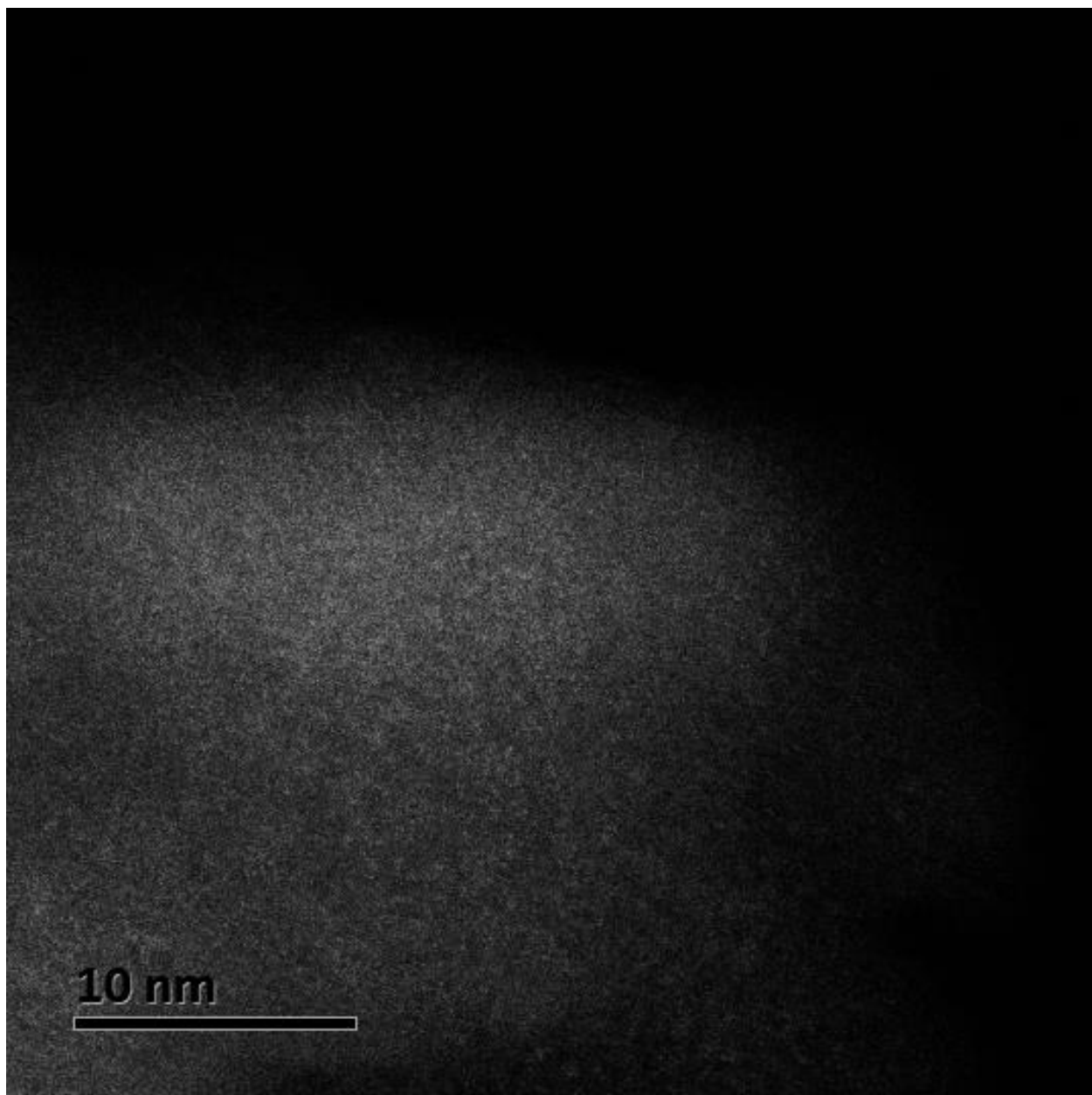


**Figure S9.** TEM images from Co-1 (scale = 10 nm).

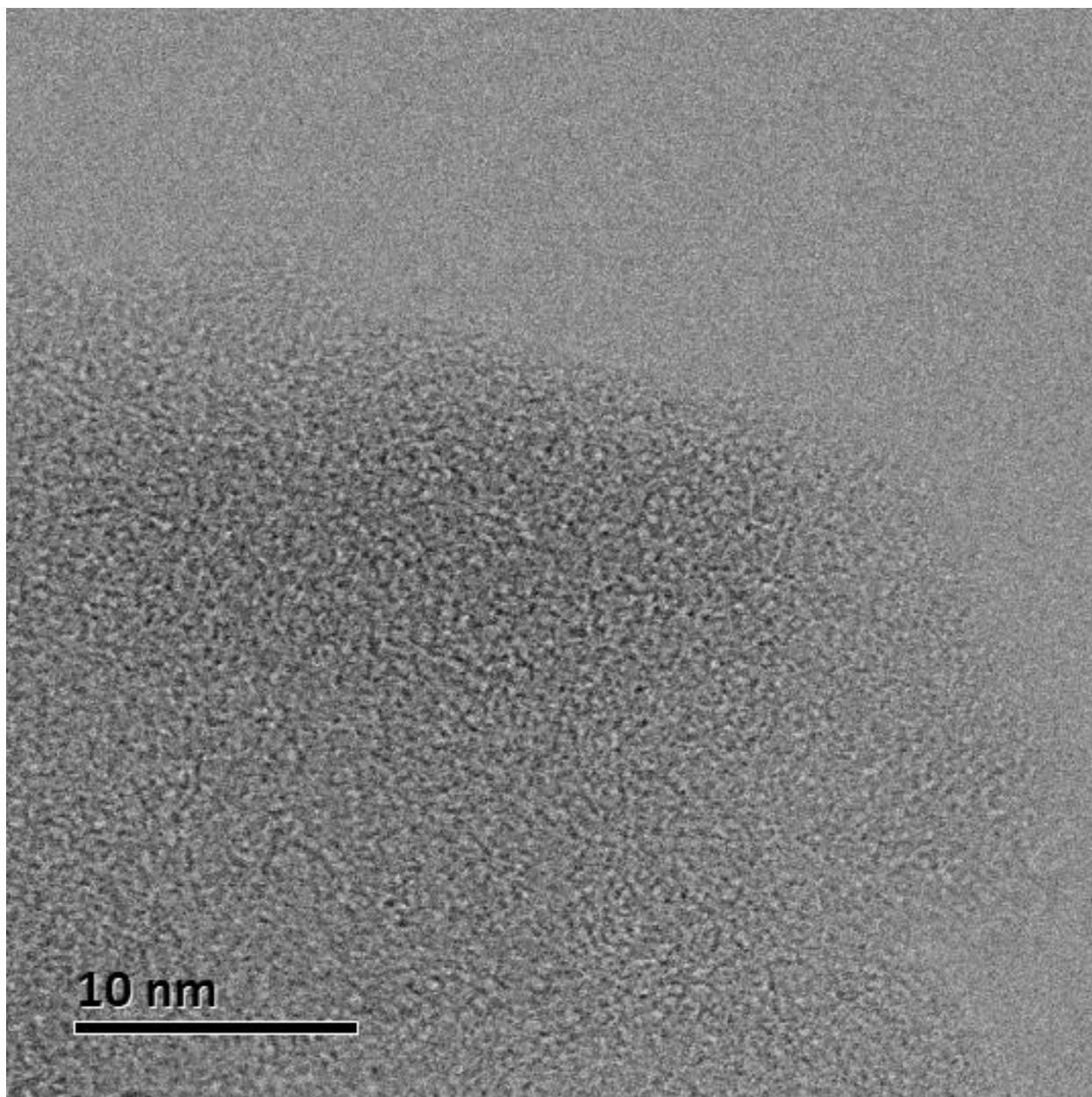


**Figure S10.** TEM images from **Co-1** (scale = 10 nm).

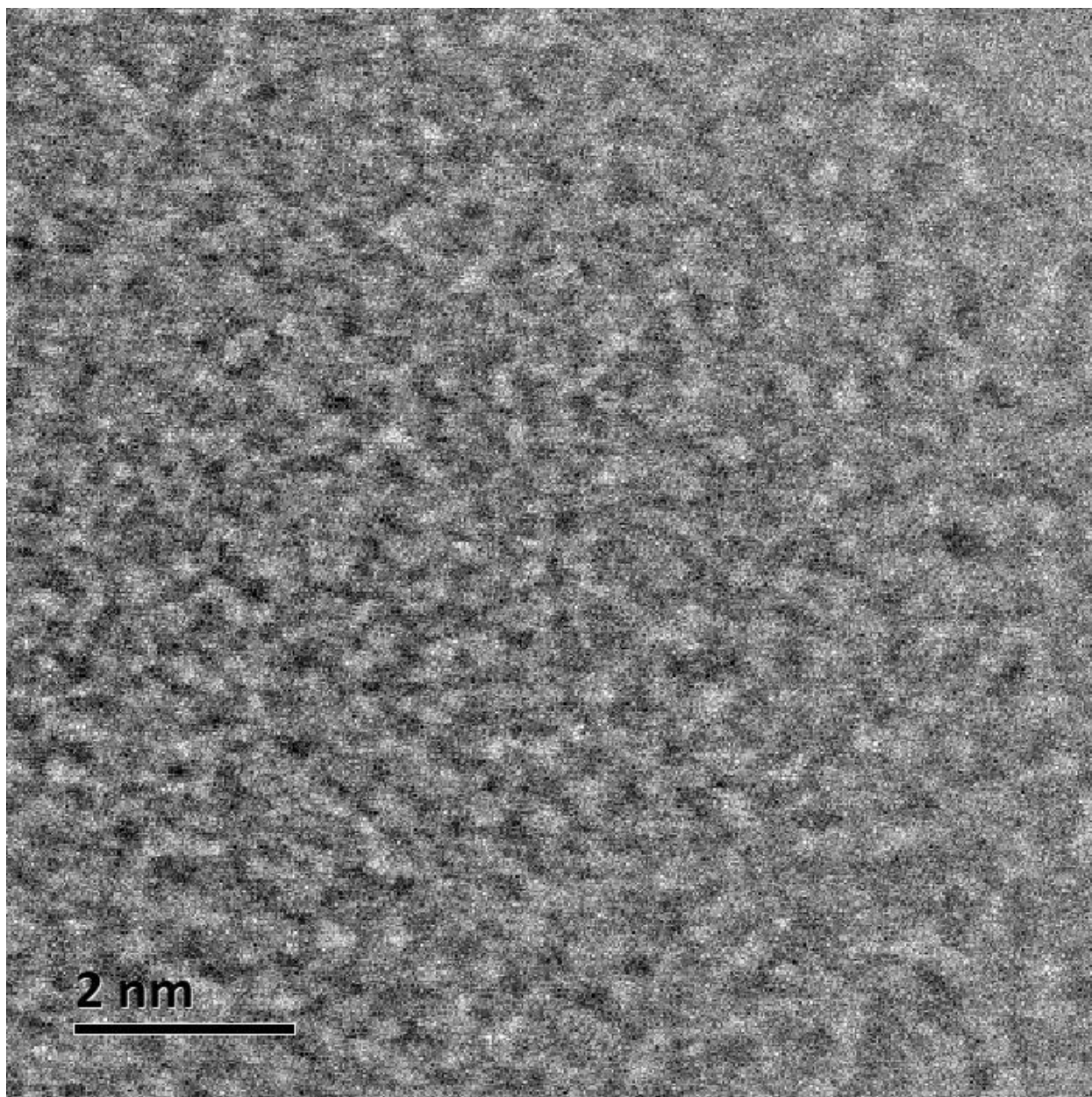


**Figure S11.** TEM images from **Co-1** (scale = 2 nm).

Co/C

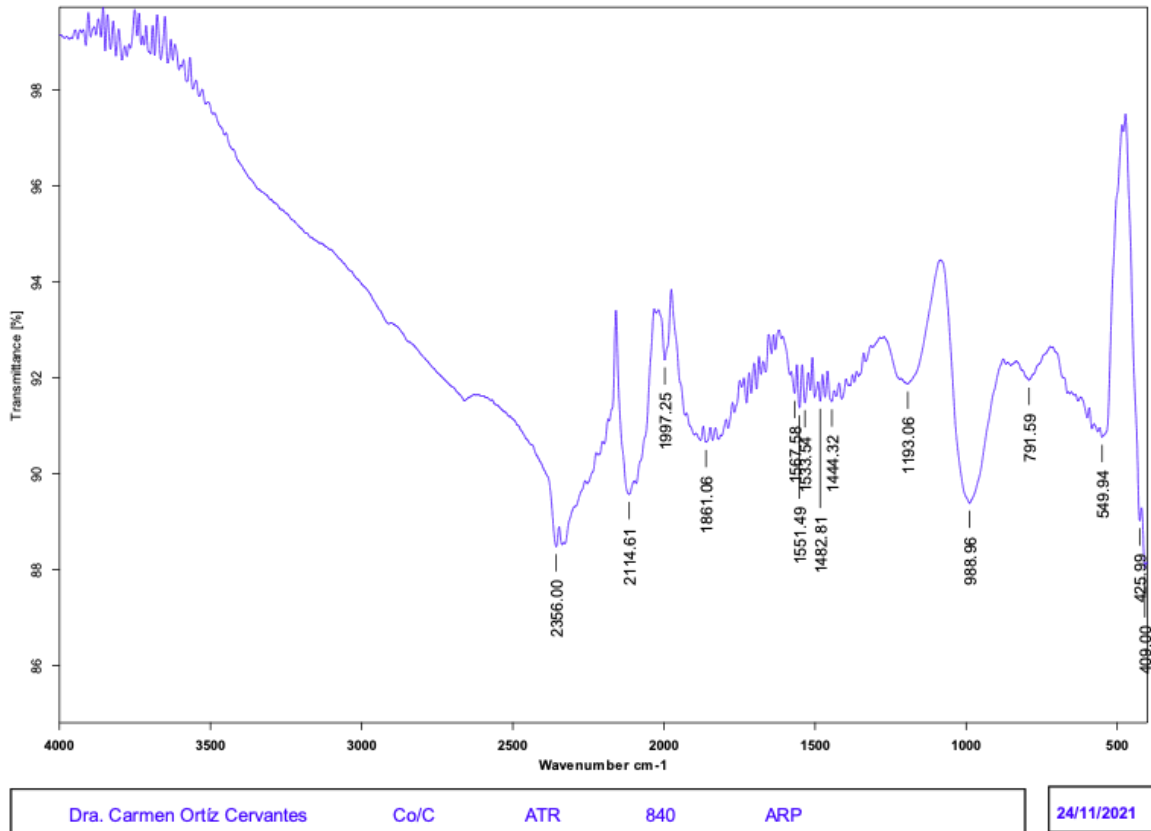
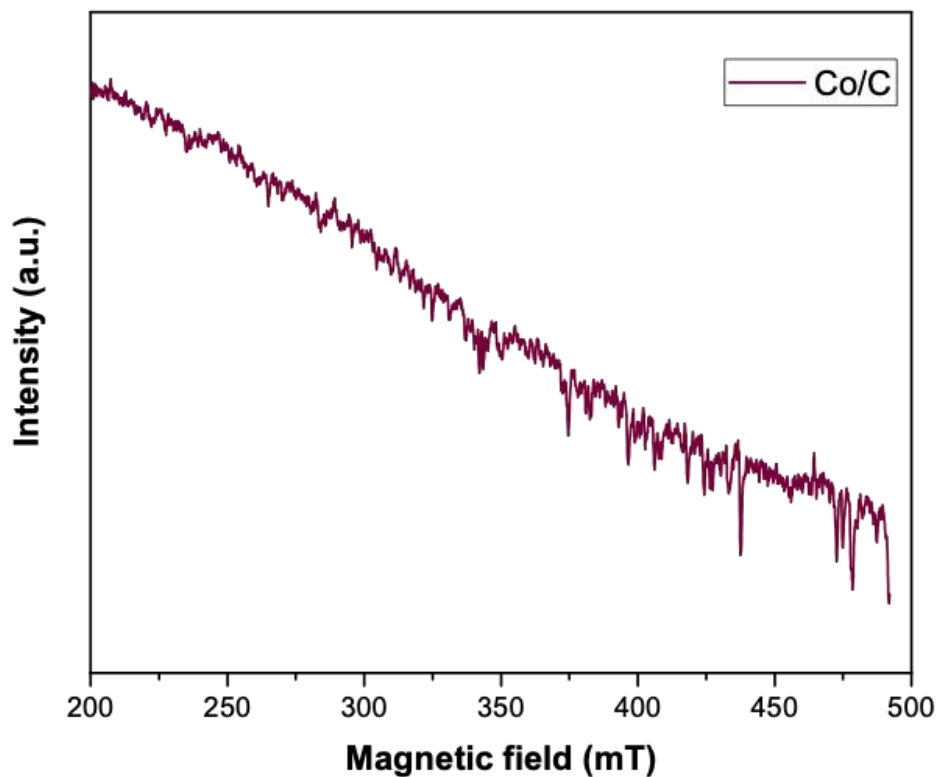


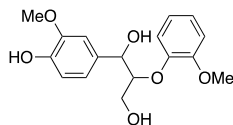
Figure S12. FTIR spectrum of Co/C.



**Figure S13.** X-band electron paramagnetic resonance (EPR) of the solid for Co/C.

### 3. Synthesis of substrates

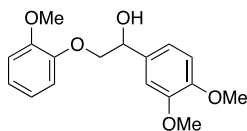
#### 3.1. Synthesis of MM-3



**Scheme 1.** Lignin model molecule, **MM-3** (guaiacylglycerol- $\beta$ -guaiacyl ether).

The **MM-3** molecule was prepared according to previously reported procedure without modification.<sup>4</sup> <sup>1</sup>H NMR (400 MHz, Chloroform-d)  $\delta$  7.13 – 6.65 (m, 7H), 5.63 (d,  $J$  = 12.5 Hz, 1H), 4.97 – 4.72 (m, 1H), 4.12 – 3.92 (m, 1H), 3.90 – 3.32 (m, 9H), 2.74 (ddd,  $J$  = 21.2, 8.0, 5.2 Hz, 1H).

### 3.2. Synthesis of **MM-2**

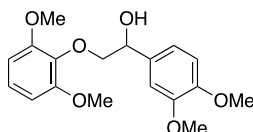


**Scheme 2.** Lignin model molecule, **MM-2**.

Compound **MM-2** was prepared according to a previously described procedure.<sup>5</sup>

**<sup>1</sup>H NMR (400 MHz, CDCl<sub>3</sub>)** δ 7.02 – 6.97 (m, 2H), 6.95 – 6.87 (m, 4H), 6.85 (d, *J* = 8.2 Hz, 1H), 5.05 (dd, *J* = 9.3, 3.0 Hz, 1H), 4.16 (dd, *J* = 10.0 Hz, 3.0 Hz), 3.97 (dd, *J* = 10 Hz, 9.7 Hz, 1H), 3.90 – 3.85 (s, 9H), 3.60 (s, 1H). **<sup>13</sup>C NMR (75 MHz, CDCl<sub>3</sub>)** δ 150.18, 149.20, 148.87, 148.12, 132.34, 122.60, 121.22, 118.73, 115.99, 112.10, 111.16, 109.54, 76.39, 72.22, 56.05, 55.99, 55.94.

### 3.3 Synthesis of **MM-1**



**Scheme 3.** Lignin model molecule, **MM-1**.

Compound **MM-1** was prepared according to a previously described procedure.<sup>6</sup>

**<sup>1</sup>H NMR (400 MHz, CDCl<sub>3</sub>)** δ 7.06 – 7.02 (m, 1H), 6.97 (m, 1H), 6.91-6.81 (m, 2H), 6.64-6.61 (m, 2H), 4.90 (dd, 2.1 Hz, 8.1 Hz, 1H), 4.54 (s, 1H), 4.40 (dd, *J* = 11.0, 2.6 Hz, 1H), 3.87 (d, *J* = 9.1 Hz, 9H), 3.86 (3, 3H), 3.70 (dd, *J* = 10.9 Hz, 10.1 Hz, 1H). **<sup>13</sup>C{<sup>1</sup>H} NMR (101 MHz, CDCl<sub>3</sub>)** δ 153.25, 148.98, 148.52, 136.80, 132.00, 124.09, 118.66, 110.93, 109.39, 105.13, 80.15, 72.22, 56.11, 55.92, 55.87.

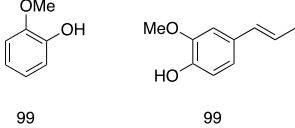
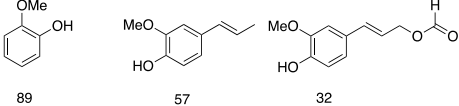
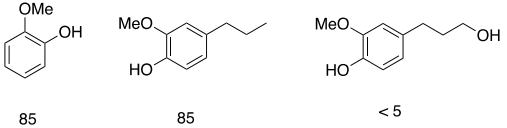
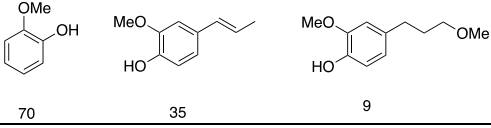
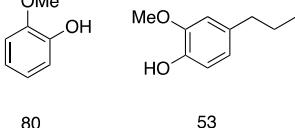
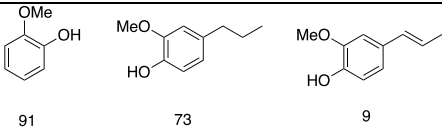
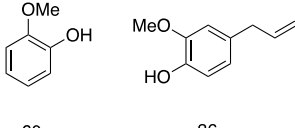
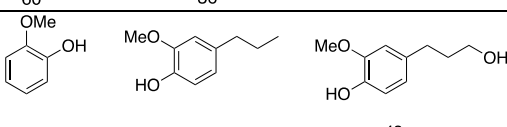
## 4. Synthesis of Co/C synthesis

The **Co/C** catalyst were prepared similarly to a procedure reported by Beller group.<sup>7</sup> Briefly, a 50 mL round bottom flask was charged with Co(acac)<sub>2</sub> (0.5 mmol) and 20 mL of ethanol and stirred for 10 min at room temperature. To this solution, 1,10-phenantroline (0.182 g, 1 mmol) was added and stirred for 120 min at 60 °C. Carbon activated (0.696 g) was added, the resulting suspension was stirred at room temperature for 18 h. The solvent was removed under reduced pressure and dried for 8 h. The resulting solid was ground in an Agate mortar, and the fine powder was transferred to a crucible with a lid and pyrolyzed at 800 °C for 2 h under nitrogen atmosphere.



## 5. Catalytic hydrogenolysis

**Table S2.** Overview of catalysts for C-O bond cleavage guaiacil-glycerol- $\beta$ -guaiacyl.

Catalyst	conditions	Products	Ref.
Co-1	H <sub>2</sub> O/EtOH, 2 h, 150 °C, Et <sub>3</sub> N, HCOOH	 99 99	<i>this work</i>
Ni-N-C/Ni-NPs	H <sub>2</sub> O/EtOH, 2 h, 150 °C, Et <sub>3</sub> N, HCOOH	 89 57 32	8
5wt% Zn/Pd/C	300 psi H <sub>2</sub> , MeOH, 150 °C, 2 h. Conv. 100%	 85 85 < 5	9
CuO/C	435 psi H <sub>2</sub> , MeOH, 200 °C, 4 h. Conv. 50.2 %	 70 35 9	10
Ni SAC@N-C	iPrOH, 200 °C, 5 h. Conv. >99%	 80 53	11
Ni@ZIF-8	435 psi H <sub>2</sub> , MeOH, 260 °C, 8 h.	 91 73 9	12
Cp <sub>2</sub> TiCl <sub>2</sub> ,	THF, 22 °C, 2h, In <sup>3+</sup> (4 equiv.) TMSCl (4 equiv.)	 60 36	13
RuNZnO/C	435 psi H <sub>2</sub> , MeOH, 220 °C, 4 h.	 61 23 43	14

## 6. Spectra and chromatograms

5788\_CBustosB\_21.10.fid  
 Instituto de Química, UNAM / C. Bustos  
 Investigador: Dra. Carmen Ortiz  
 No. de registro: 5788  
 Clave:MM-3-2  
 Disolvente: CDCl<sub>3</sub>  
 Hidrogeno 1  
 Bruker Avance III 400 MHz (H)  
 Sonda BBO 400S1 BBF-H-D-052  
 14-septiembre-2021

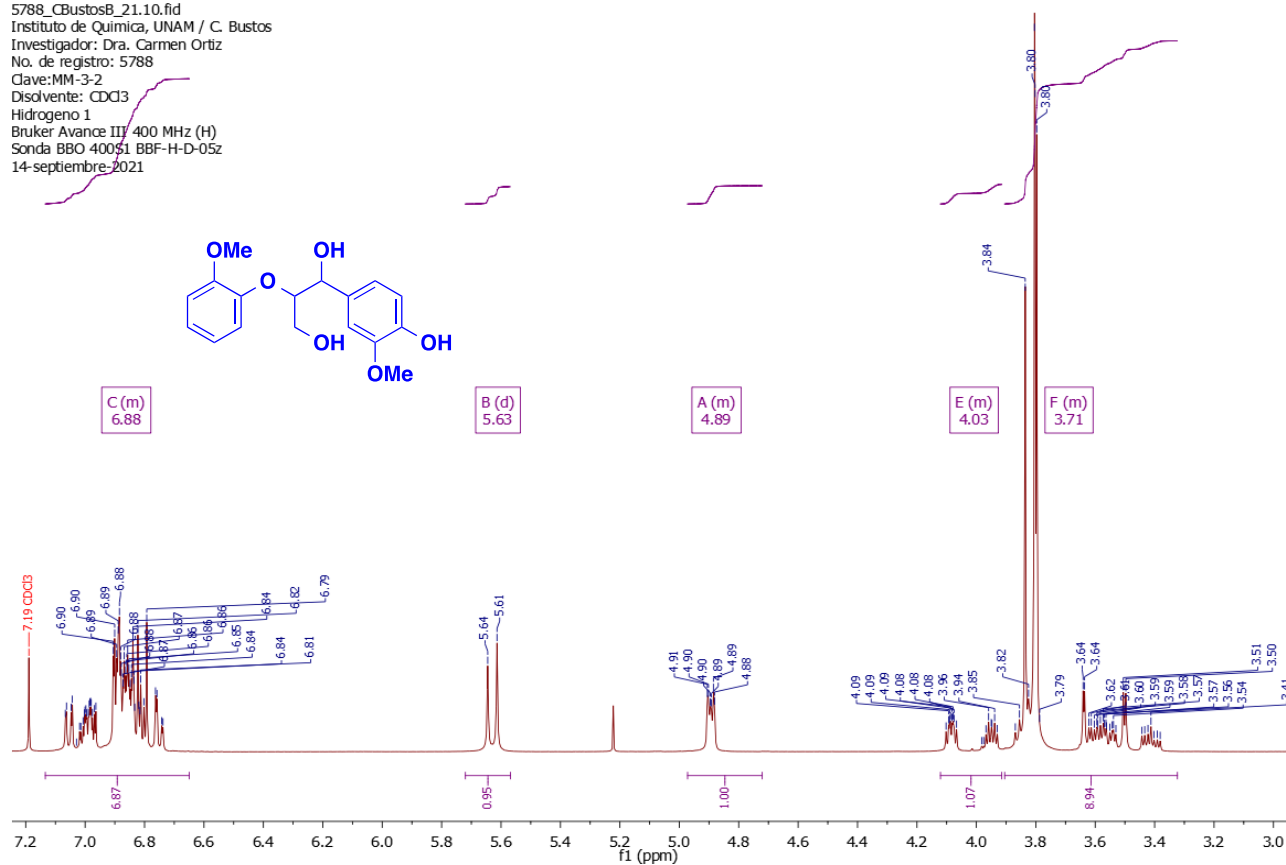


Figure S14. <sup>1</sup>H NMR (400 MHz, CDCl<sub>3</sub>) spectrum of compound MM-3.

Abundance

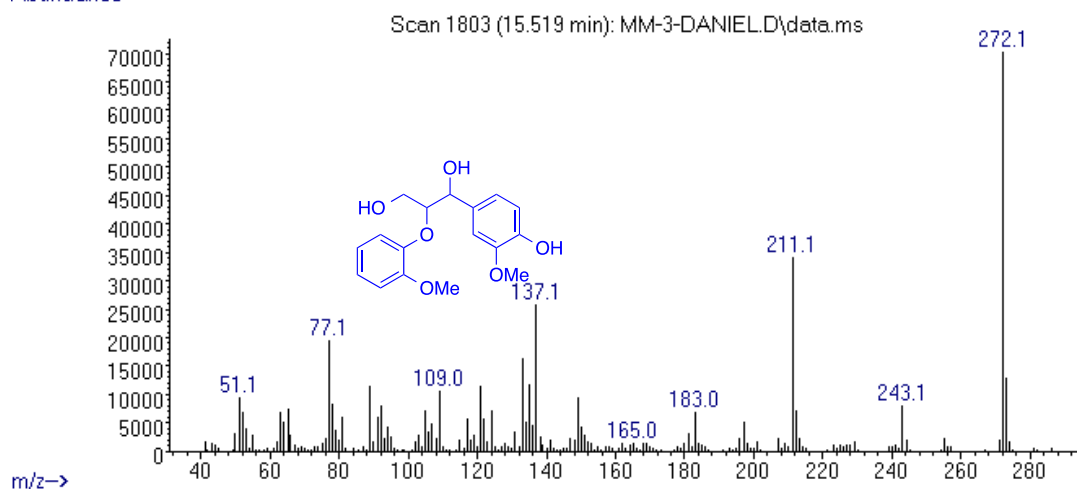


Figure S15. Mass spectrum of compound MM-3.

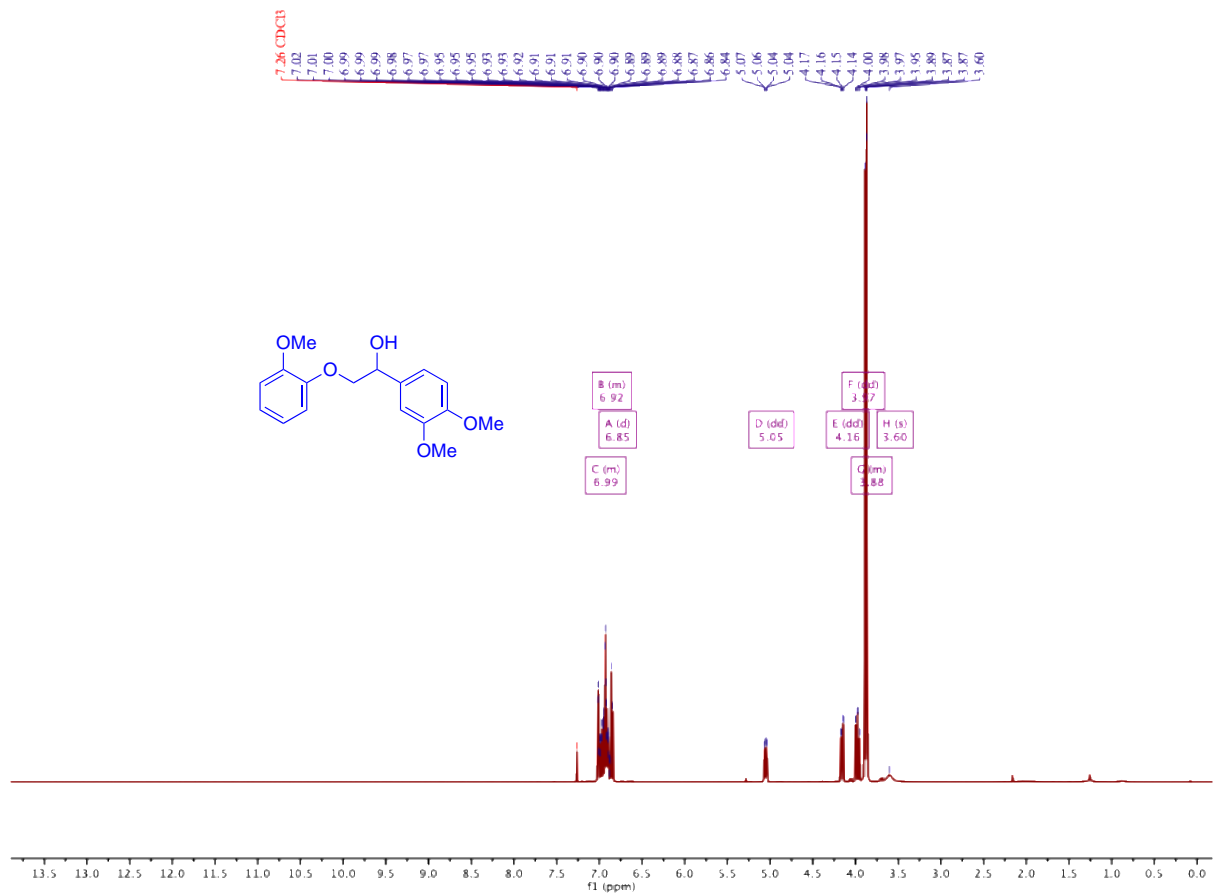
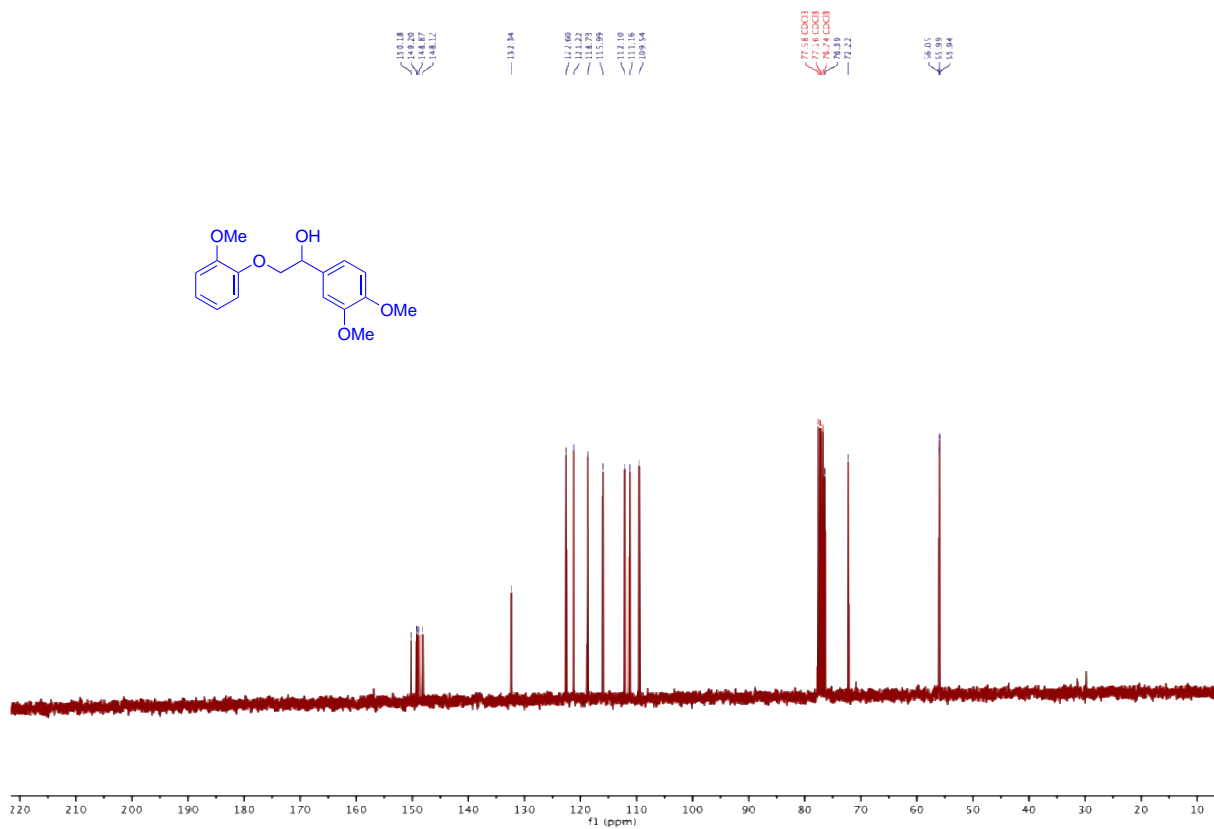


Figure S16. <sup>1</sup>H NMR (400 MHz, CDCl<sub>3</sub>) of compound MM-2.



**Figure S17.**  $^{13}\text{C}\{^1\text{H}\}$  NMR (101 MHz,  $\text{CDCl}_3$ ) of compound MM-2.

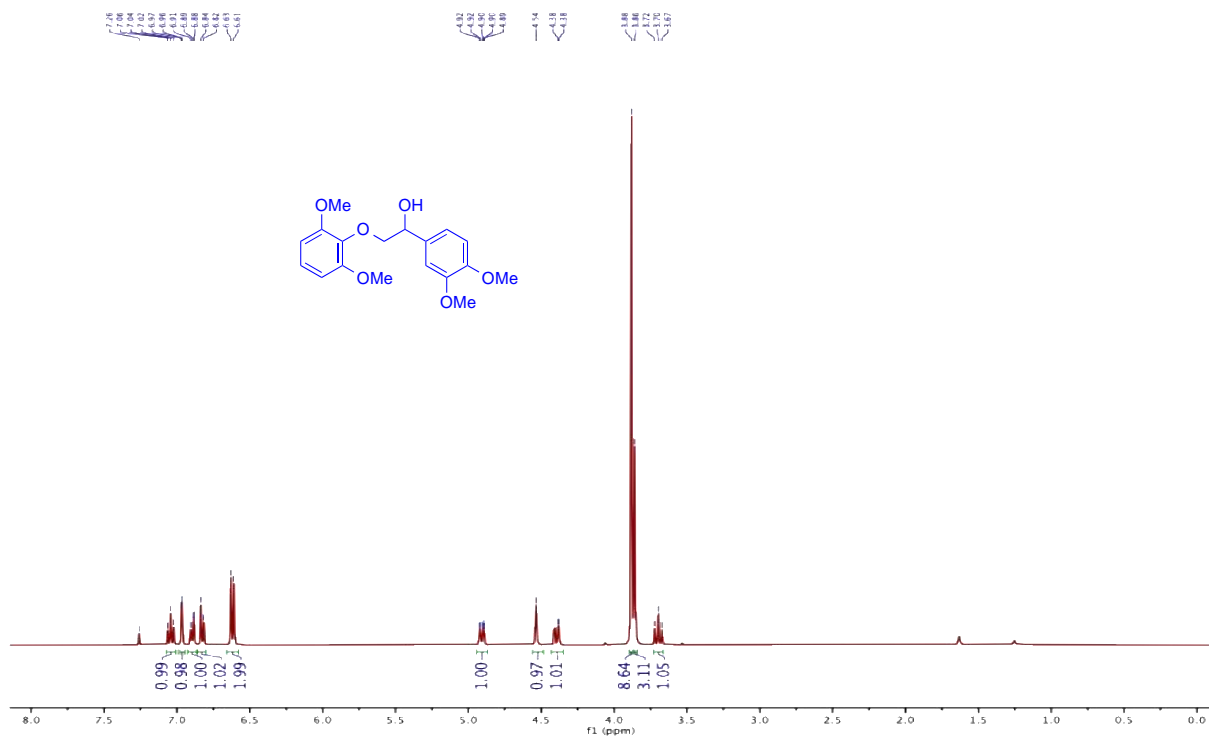


Figure S18.  $^1\text{H}$  NMR (400 MHz,  $\text{CDCl}_3$ ) of compound MM-1.

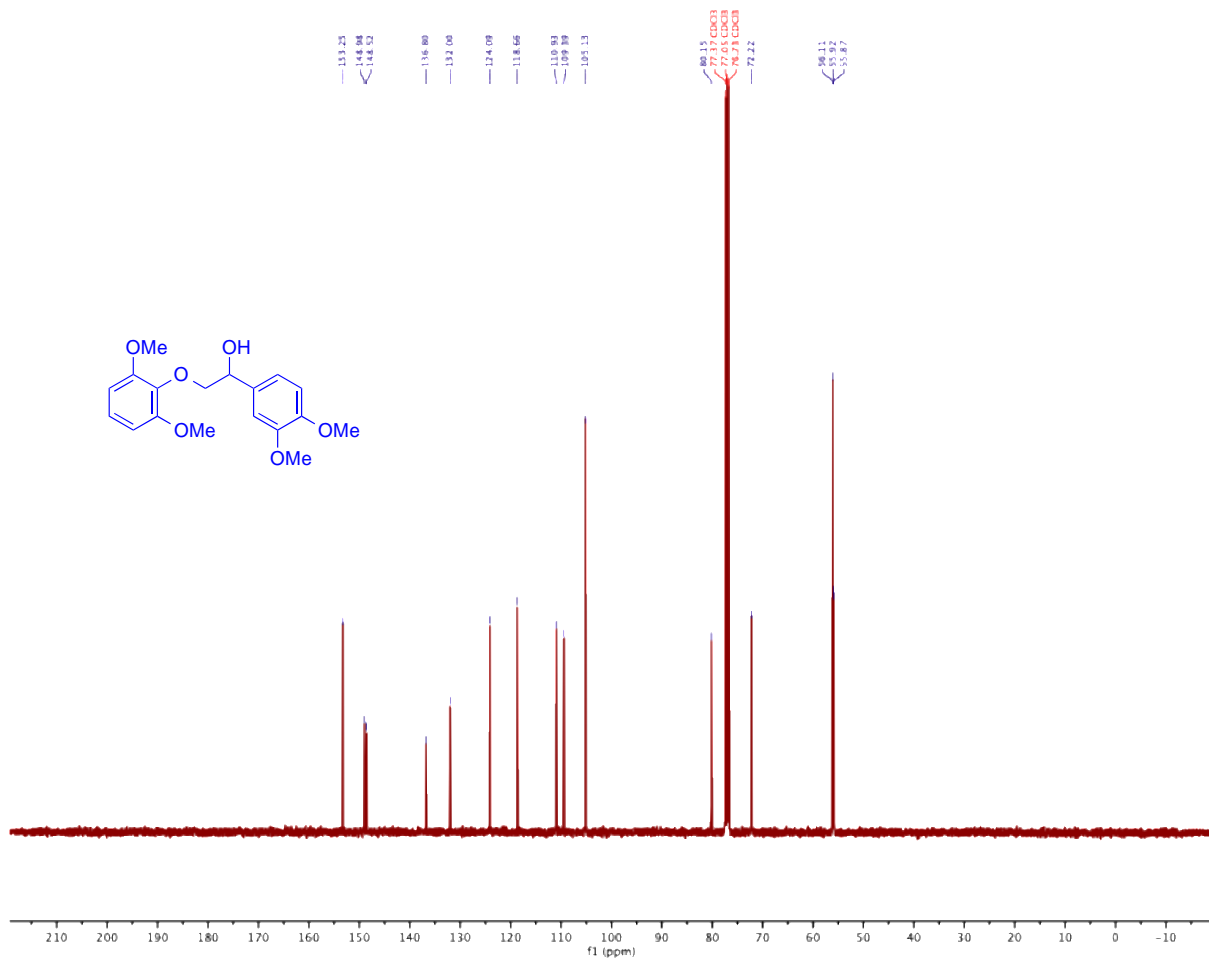


Figure S19. <sup>13</sup>C{<sup>1</sup>H} NMR (101 MHz, CDCl<sub>3</sub>) of compound MM-1.

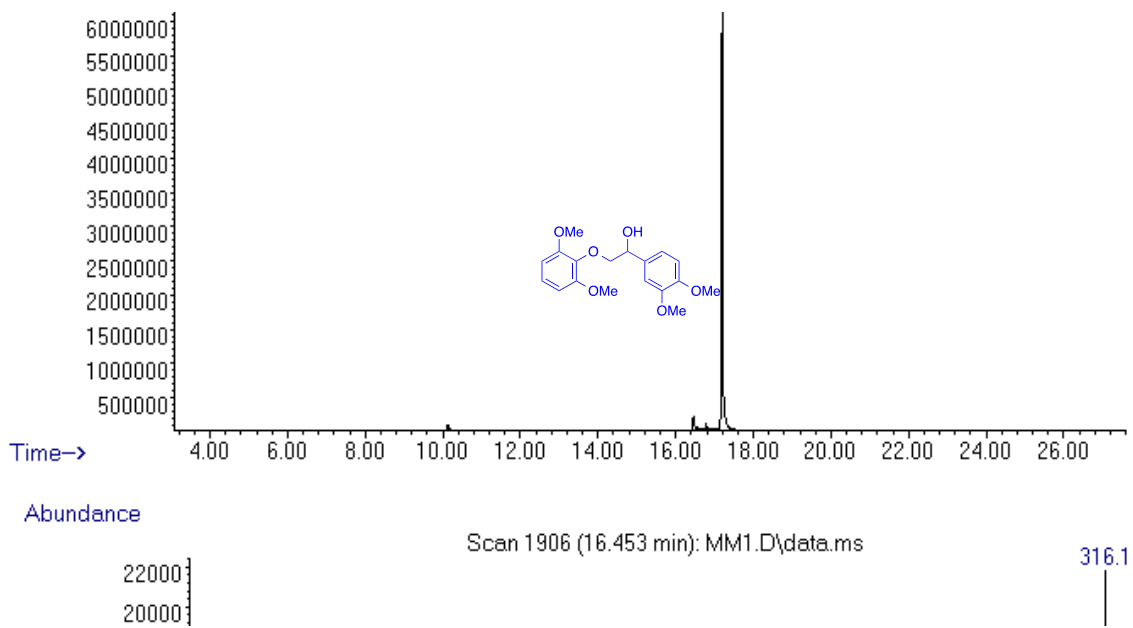


Figure S20. Chromatogram of MM-1.

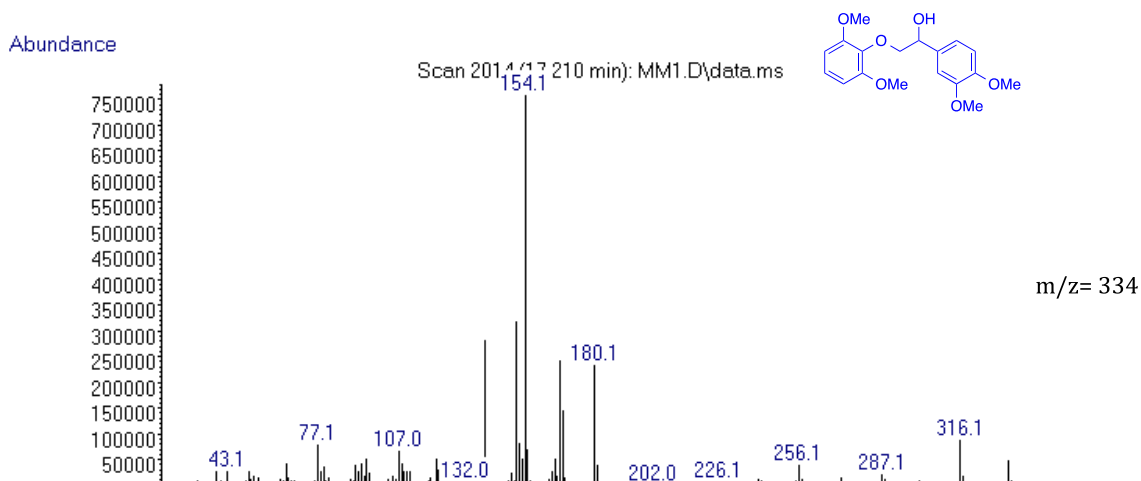


Figure S21. Electronic impact mass spectrum for compound MM-1.

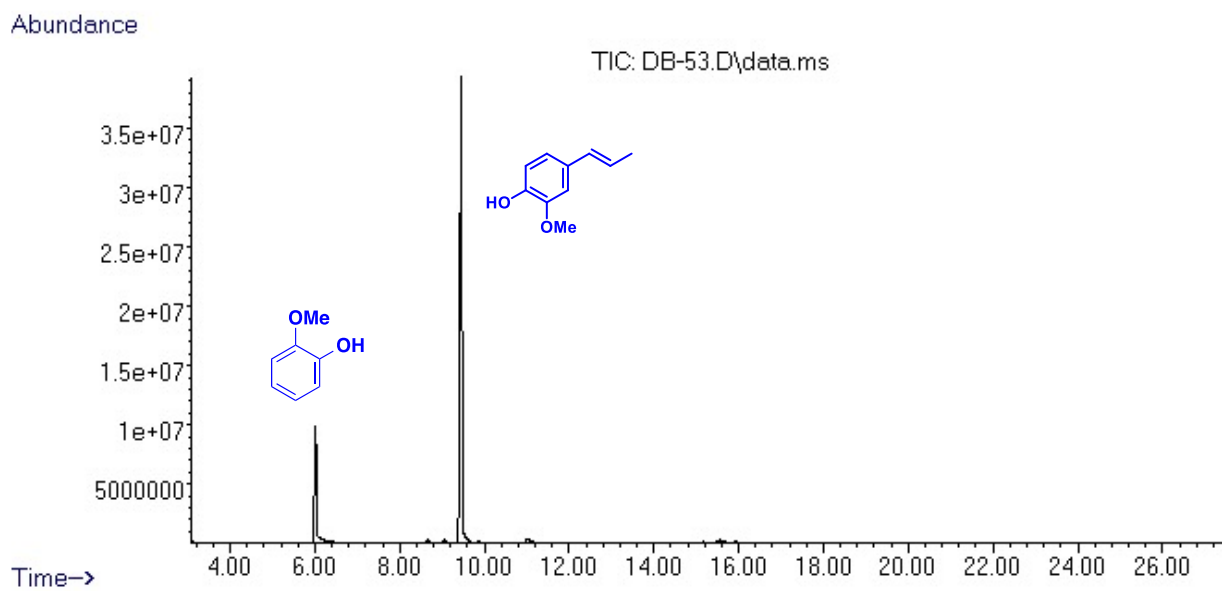
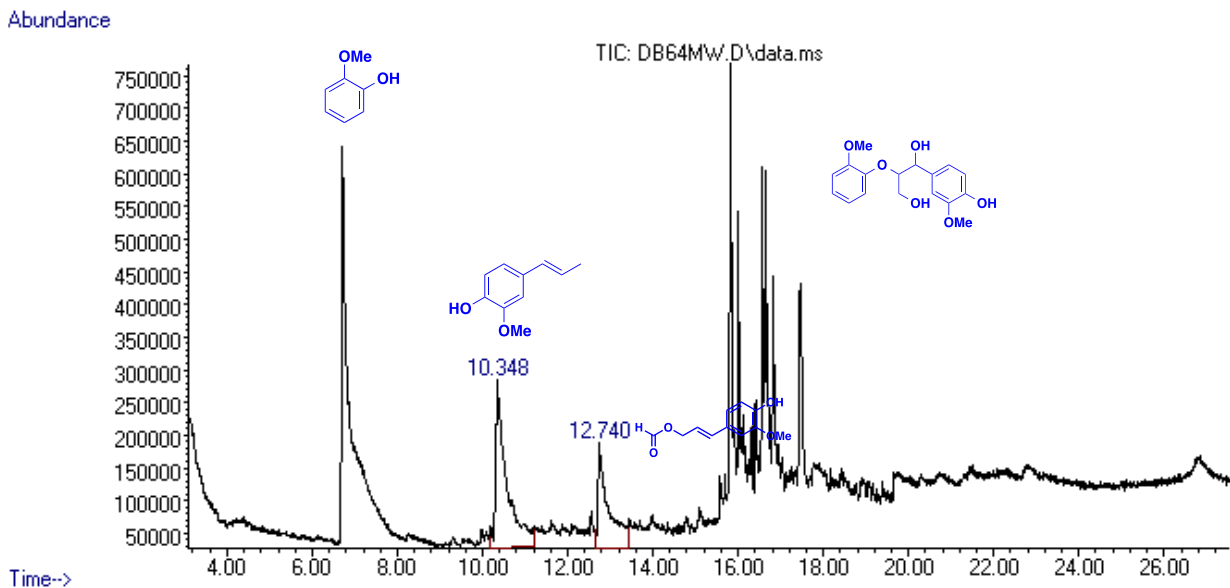
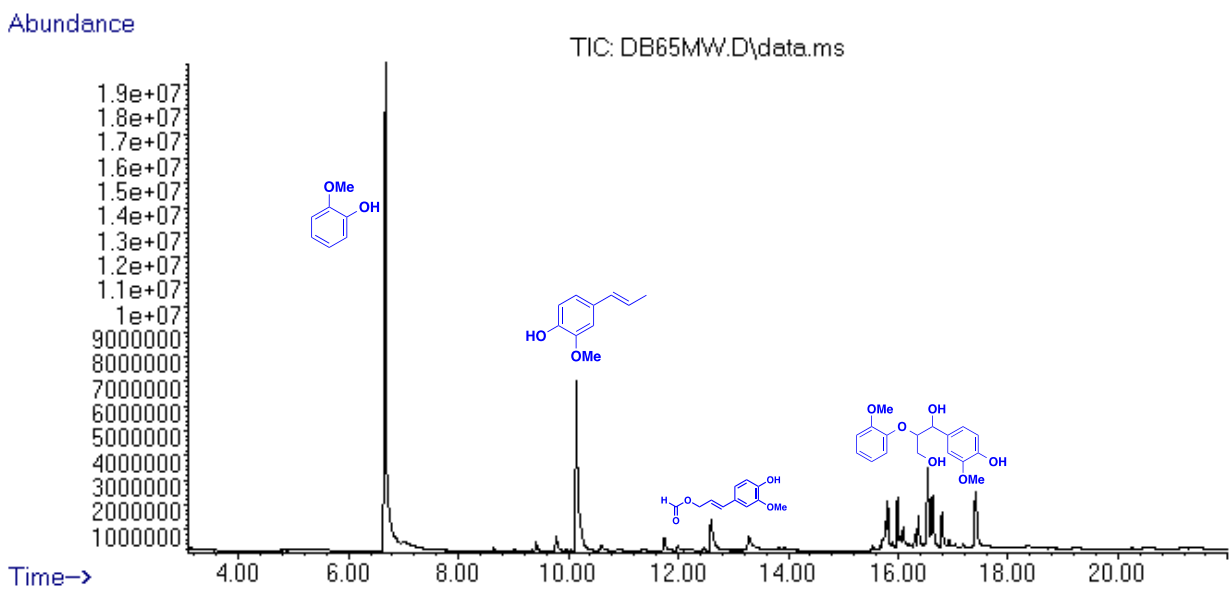


Figure S22. Chromatogram of MM-3 hydrogenolysis with Co-1.



**Figure S23.** Chromatogram of MM-3 hydrogenolysis with Co/C.



**Figure S24.** Chromatogram of MM-3 hydrogenolysis with Co-1 in presence of KSCN (10 mM).



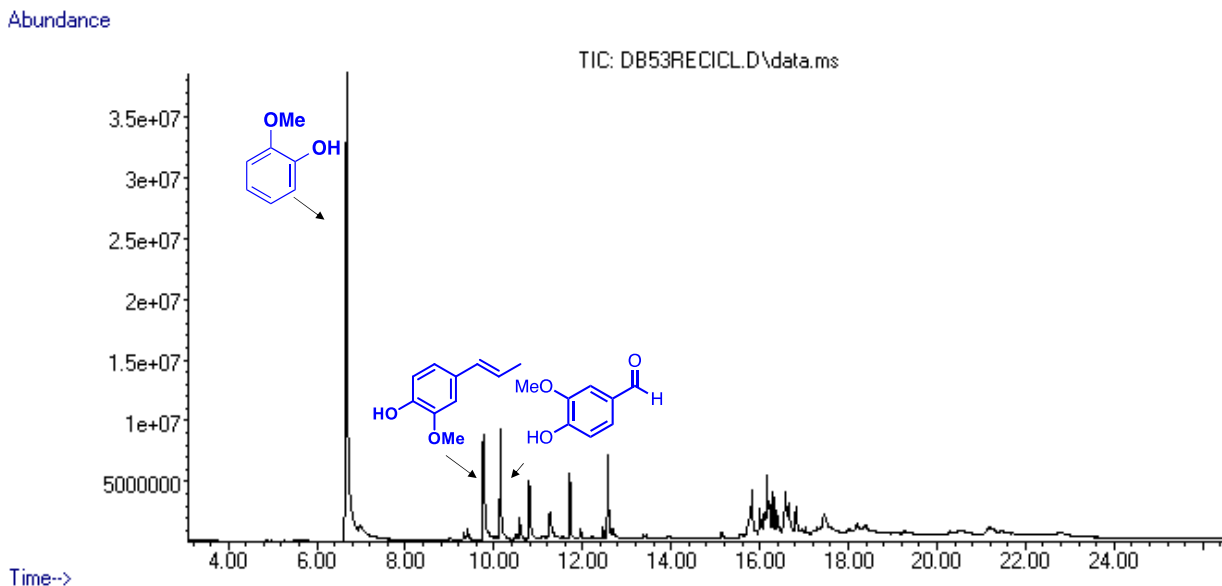


**Figure S25.** Chromatogram of MM-3 hydrogenolysis with recycled Co-1.

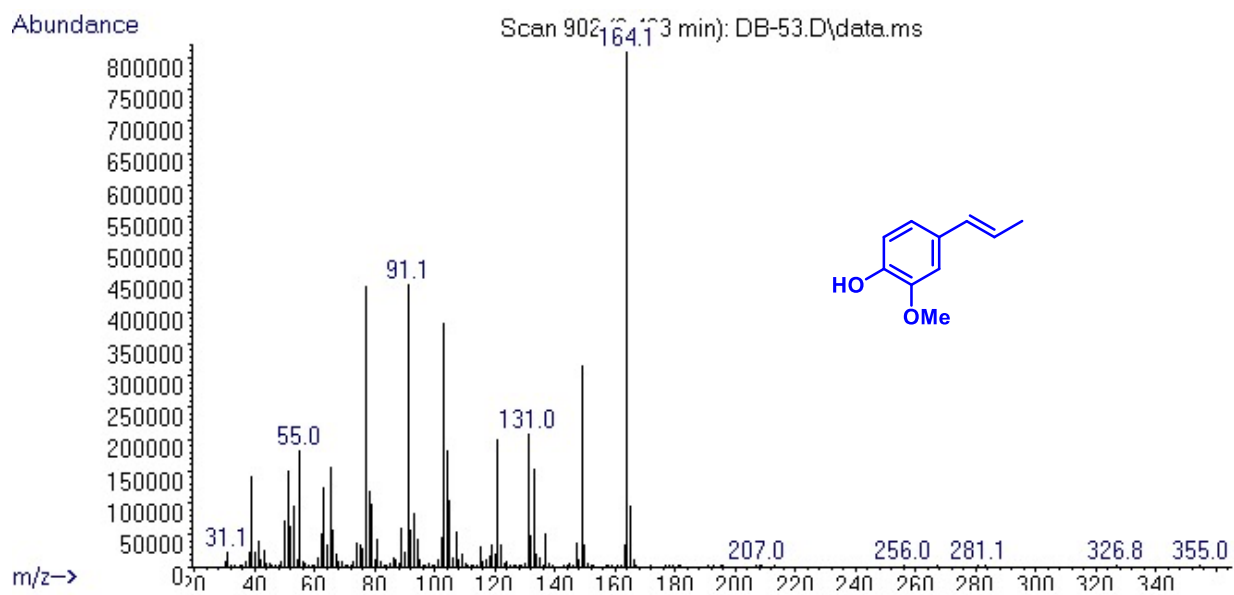


**Figure S26.** Electronic impact mass spectrum for compound **iso Eugenol** (2-methoxy-4-[(E)-1-propenyl] phenol).

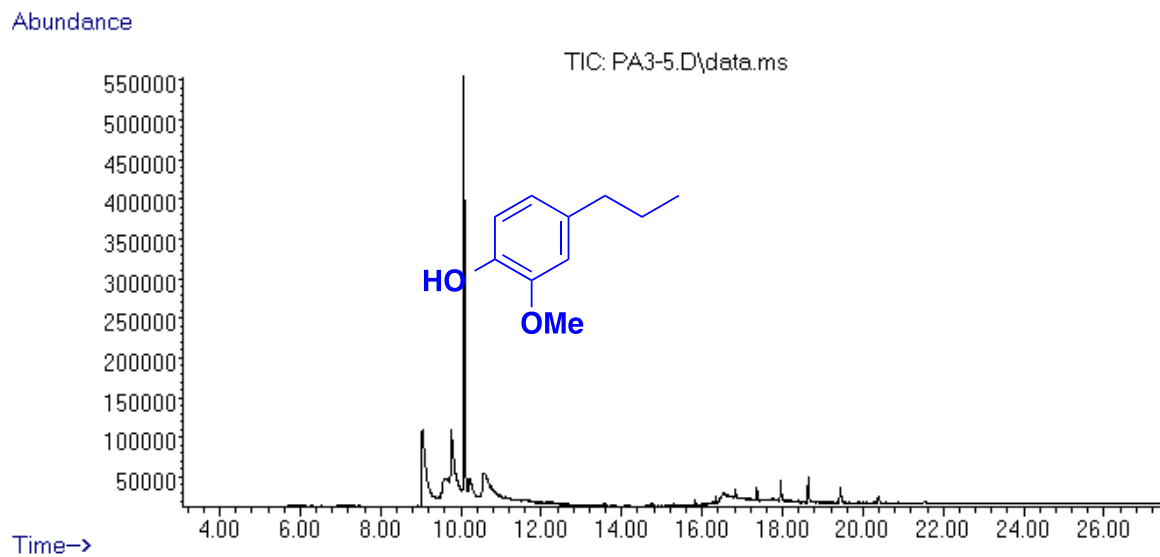


**Figure S27.** Electronic impact mass spectrum for **2-methoxy-4-propyl phenol**.

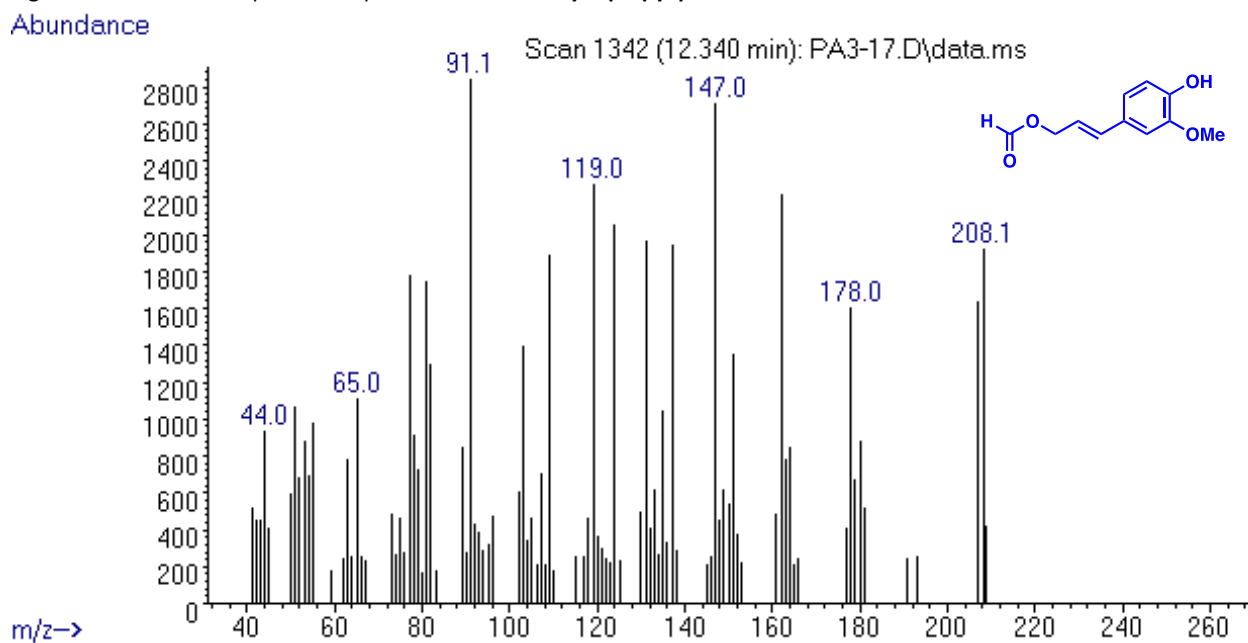


**Figure S28.** Electronic impact mass spectrum for **(E)-4-(3-ethoxyprop-1-en-1-yl)-2-methoxyphenol**.

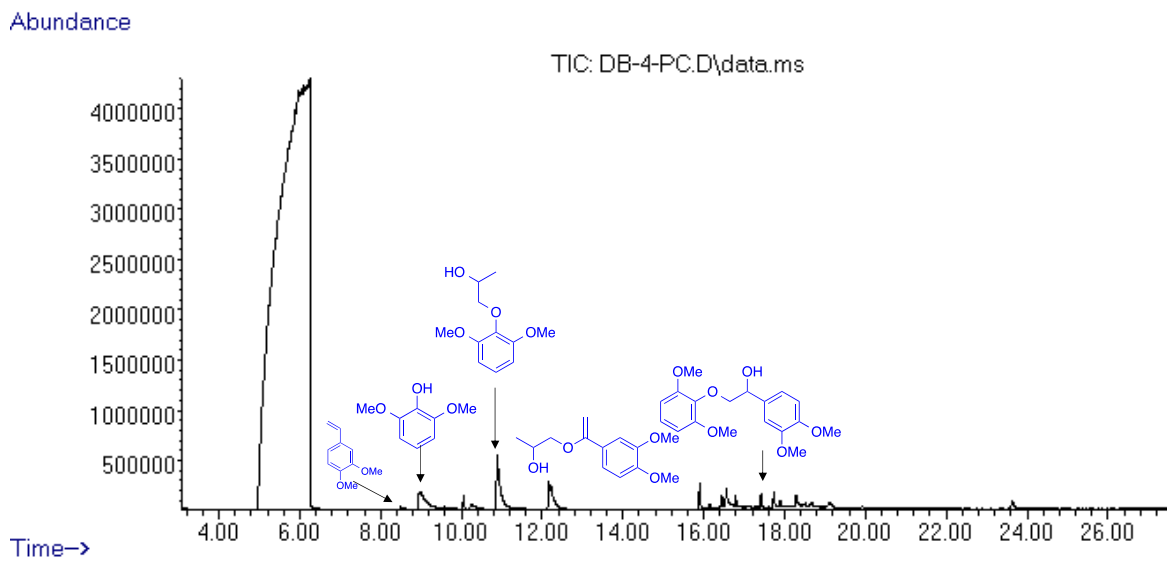


**Figure S29.** Chromatogram of **MM-1** hydrogenolysis with propylene carbonate as solvent.

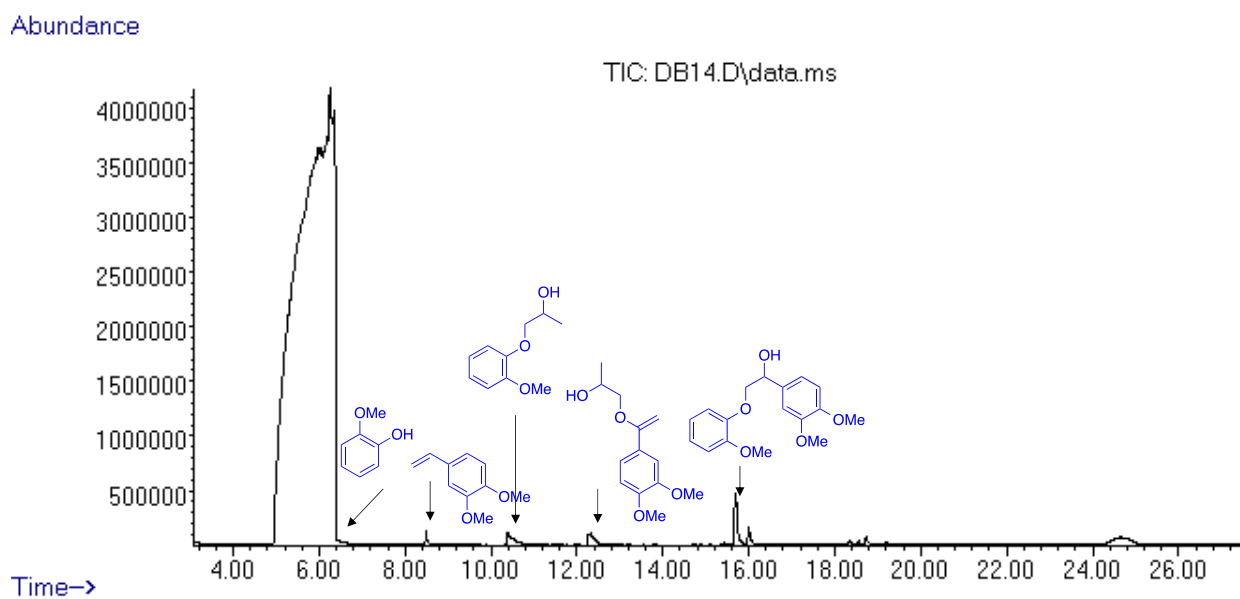


**Figure S30.** Chromatogram of **MM-2** hydrogenolysis with **Co-1** catalyst and propylene carbonate as solvent.

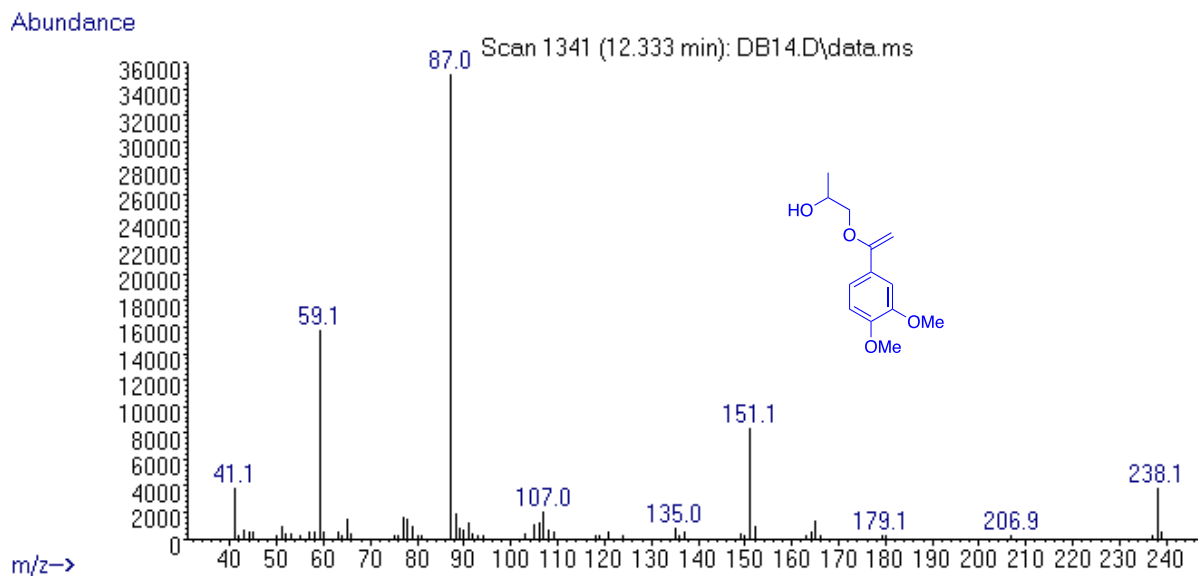


**Figure S31.** Electronic impact mass spectrum for 1-((1-(3,4-dimethoxyphenyl) vinyl)oxy)propan-2-ol.

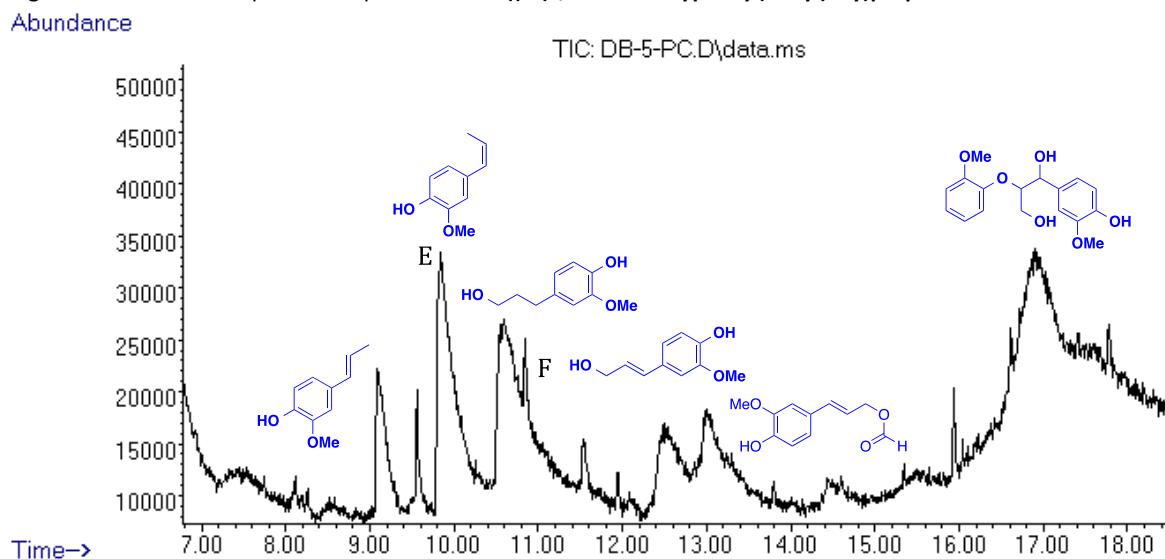


**Figure S32.** Chromatogram of MM-3 hydrogenolysis with Co-1 catalyst and propylene carbonate as solvent.

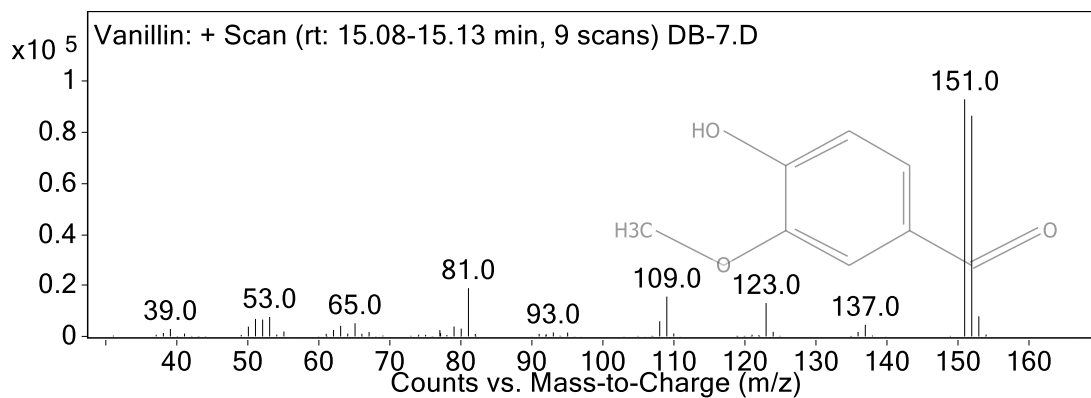


**Figure S33.** Electronic impact mass spectrum for vanillin.

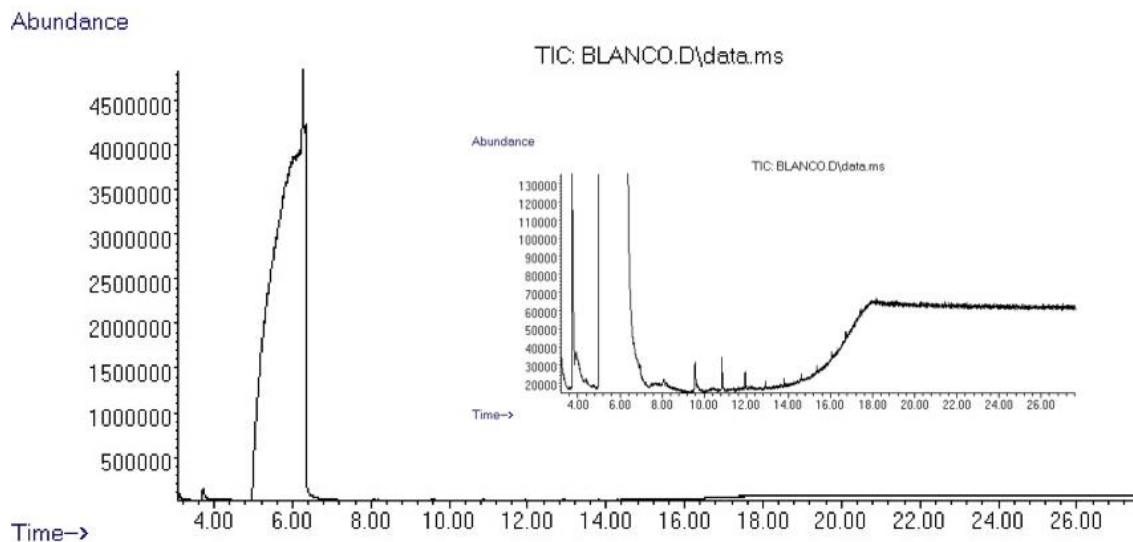


Figure S34. Chromatogram of MM-3 hydrogenolysis without catalyst.

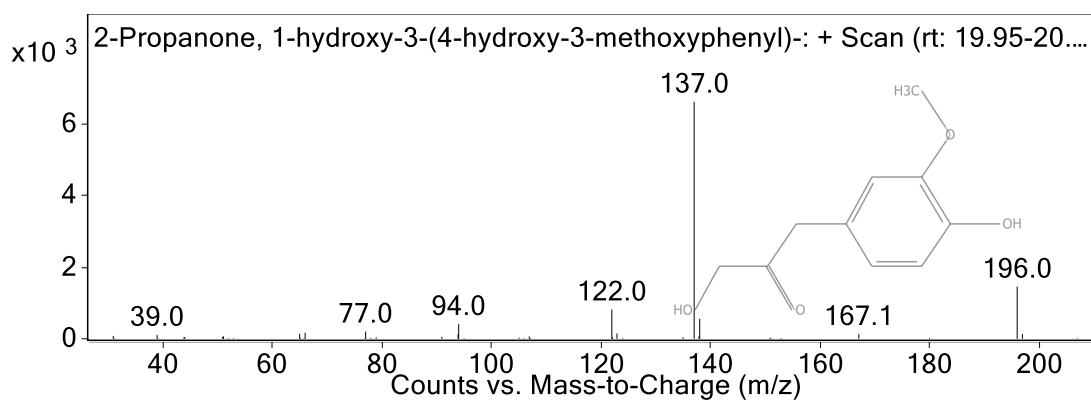


Figure S35. Electronic impact mass spectrum for 1-hydroxy-3-(4-hydroxy-3-methoxyphenyl)-2-propanone.

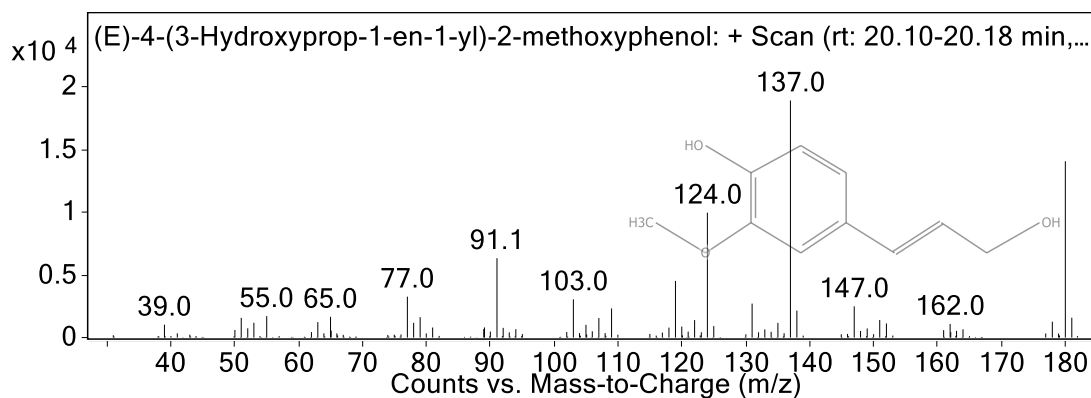
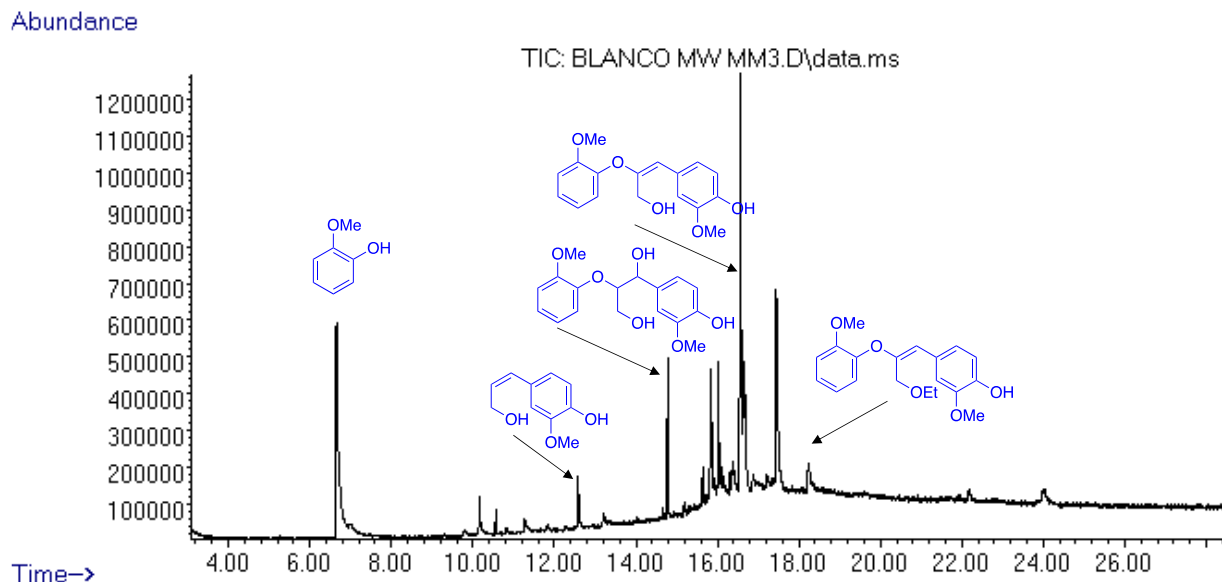
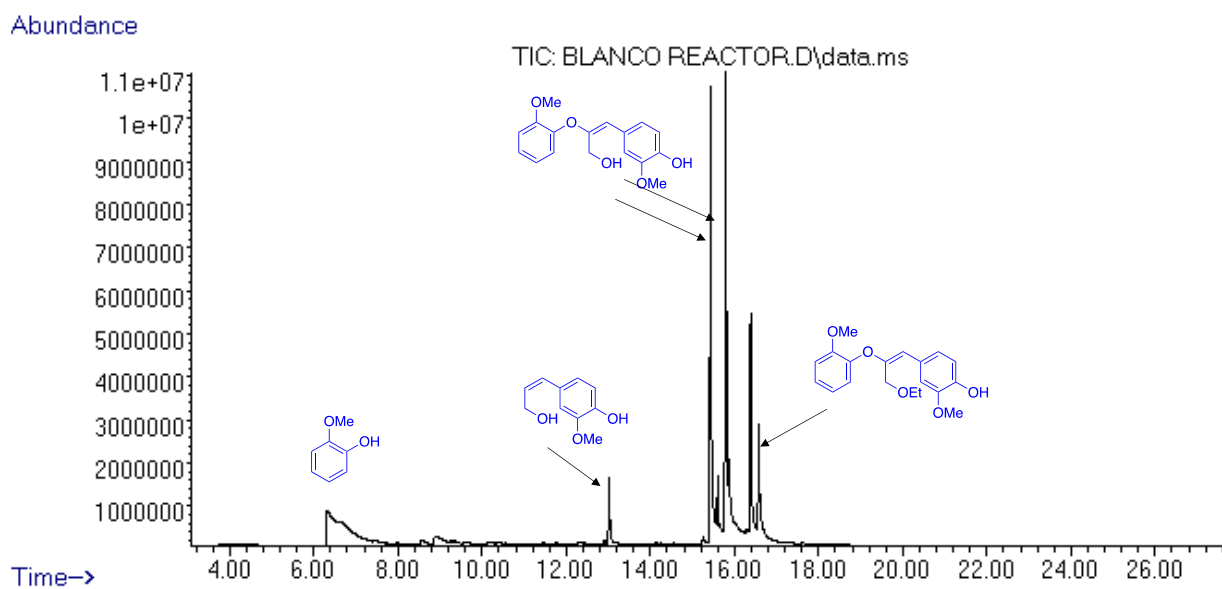


Figure S36. Electronic impact mass spectrum for (E)-4-(3-hydroxyprop-1-en-1-yl)-2-methoxyphenol.



**Figure S37.** Chromatogram of **MM-3** hydrogenolysis in EtOH/water with  $\text{Et}_3\text{N}/\text{HCOOH}$  without catalyst at 150 °C for 2h.



**Figure S38.** Chromatogram of **MM-3** hydrogenolysis in EtOH/water with  $\text{Et}_3\text{N}/\text{HCOOH}$  without catalyst at 150 °C for 24 h.

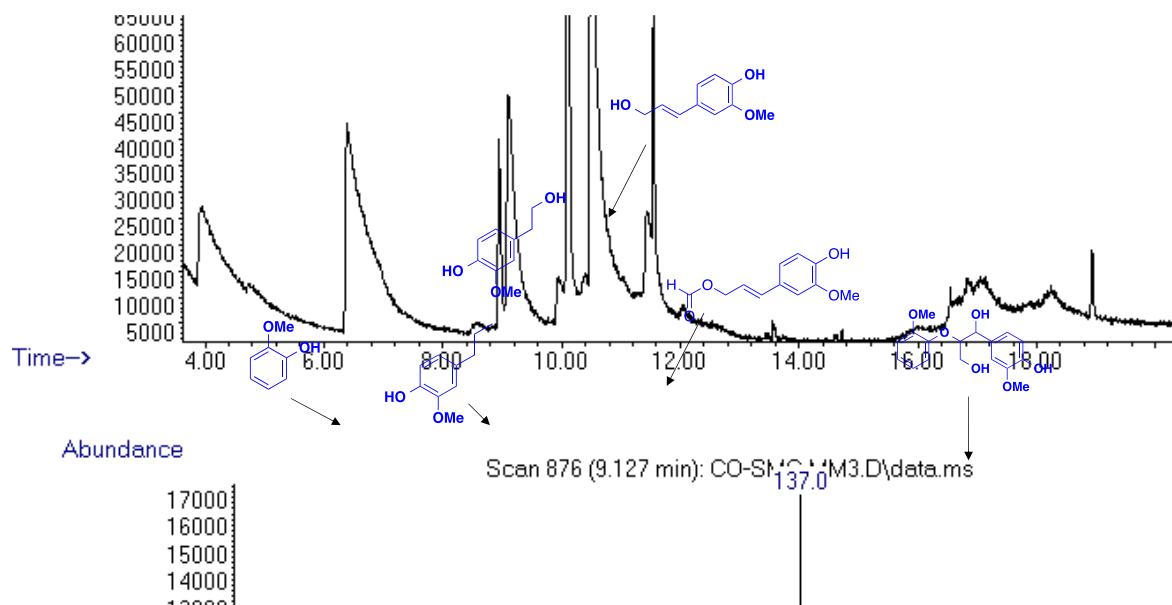


**Figure S39.** Chromatogram of **MM-3** hydrogenolysis in EtOH/water with HCOOH and without Et<sub>3</sub>N with **Co-2** at 150 °C for 24 h.

Abundance

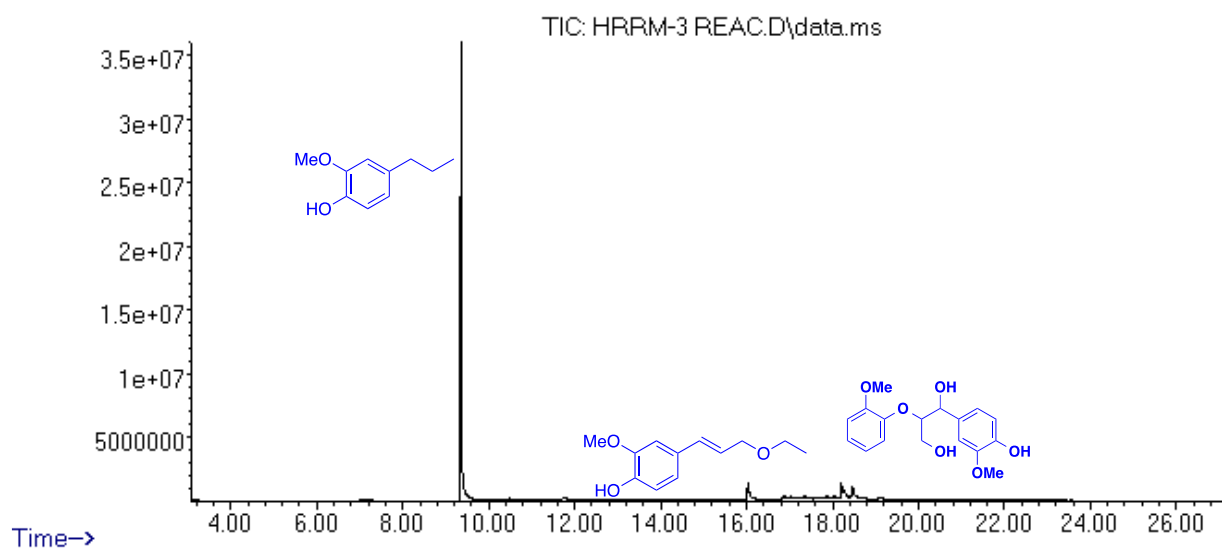


**Figure S40.** Chromatogram of **MM-3** hydrogenolysis in EtOH/water, H<sub>2</sub> (10 bar) with **Co-2** at 150 °C for 24 h.

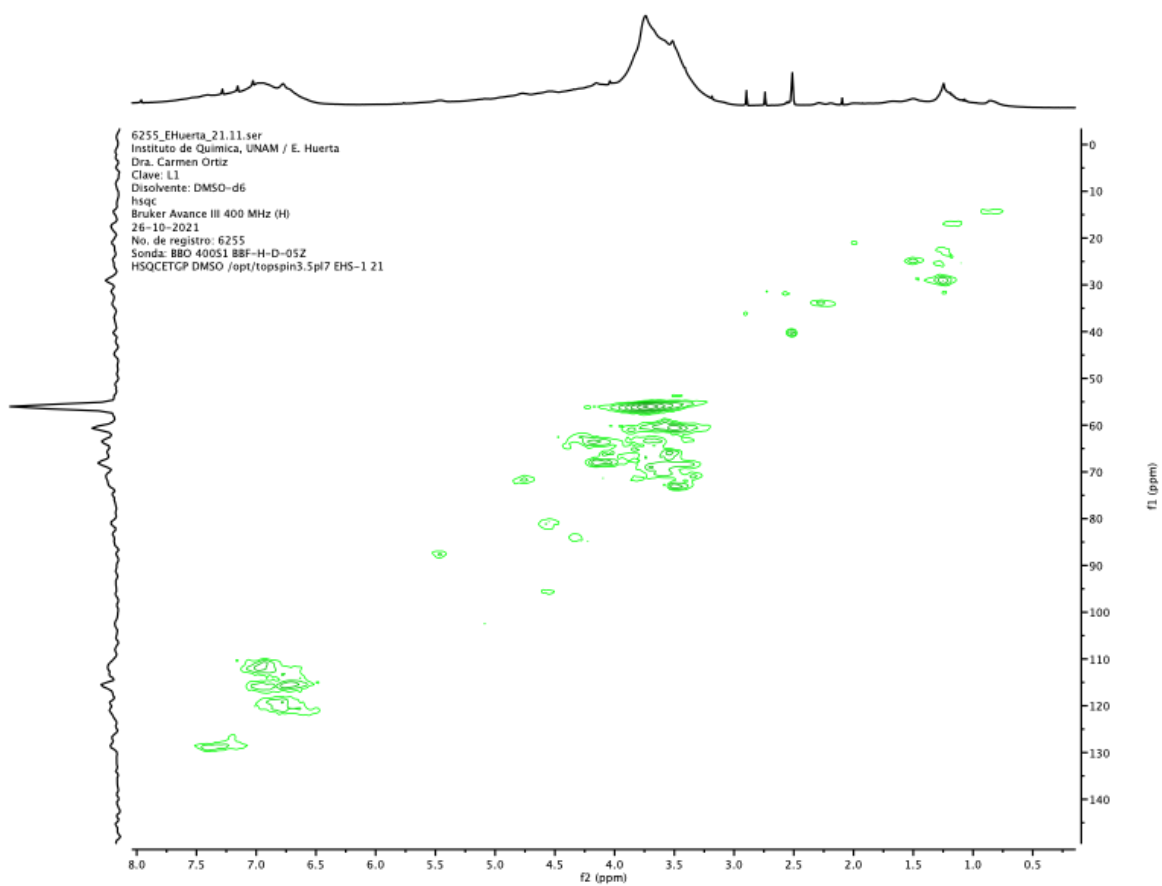
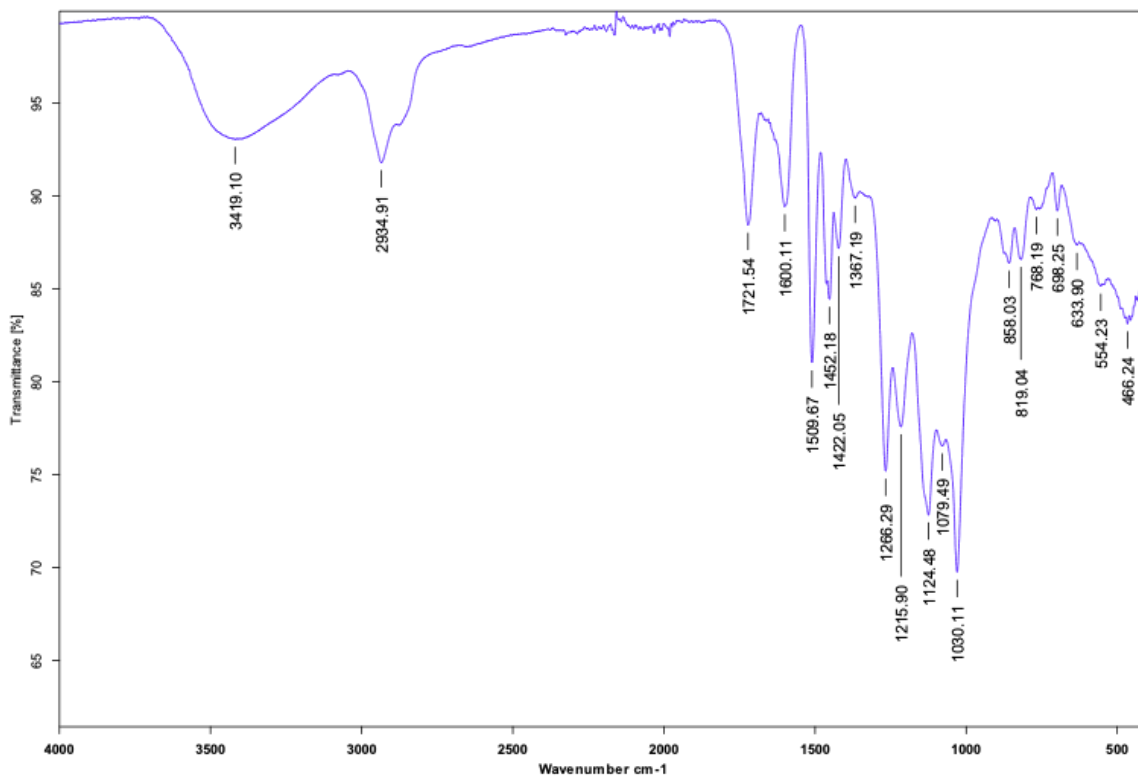


**Figure S41.**  $^1\text{H}$ - $^{13}\text{C}$  gHSQC NMR (DMSO-d<sub>6</sub>, 400 MHz) of pine dioxasolv lignin.





Dra. Carmen Ortiz                      Li                      ATR                      585                      ARP                      07/10/2021

Figure S42. FTIR spectrum of pine dioxasolv lignin.

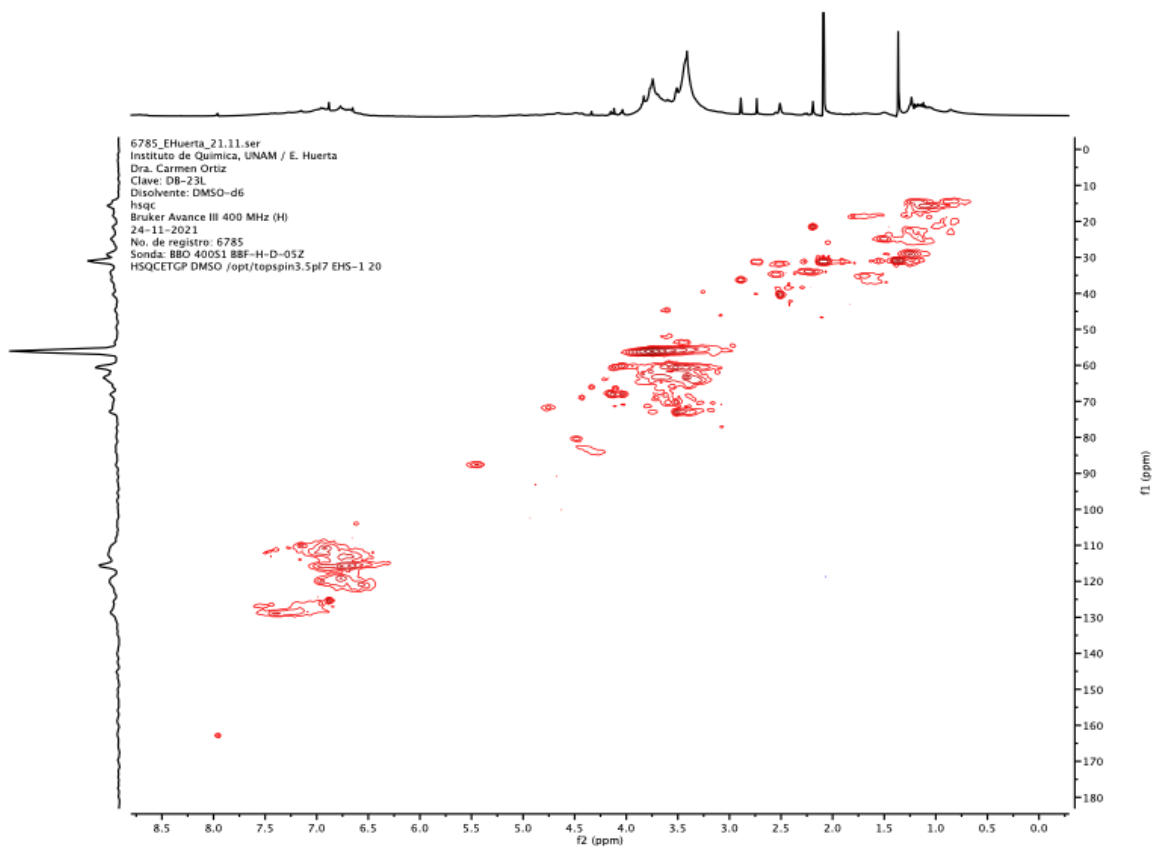


**Figure S43.**  $^1\text{H}$ - $^{13}\text{C}$  gHSQC NMR (DMSO- $d_6$ , 400 MHz) of hydrogenolysis of dioxasolv lignin with **Co-1**.

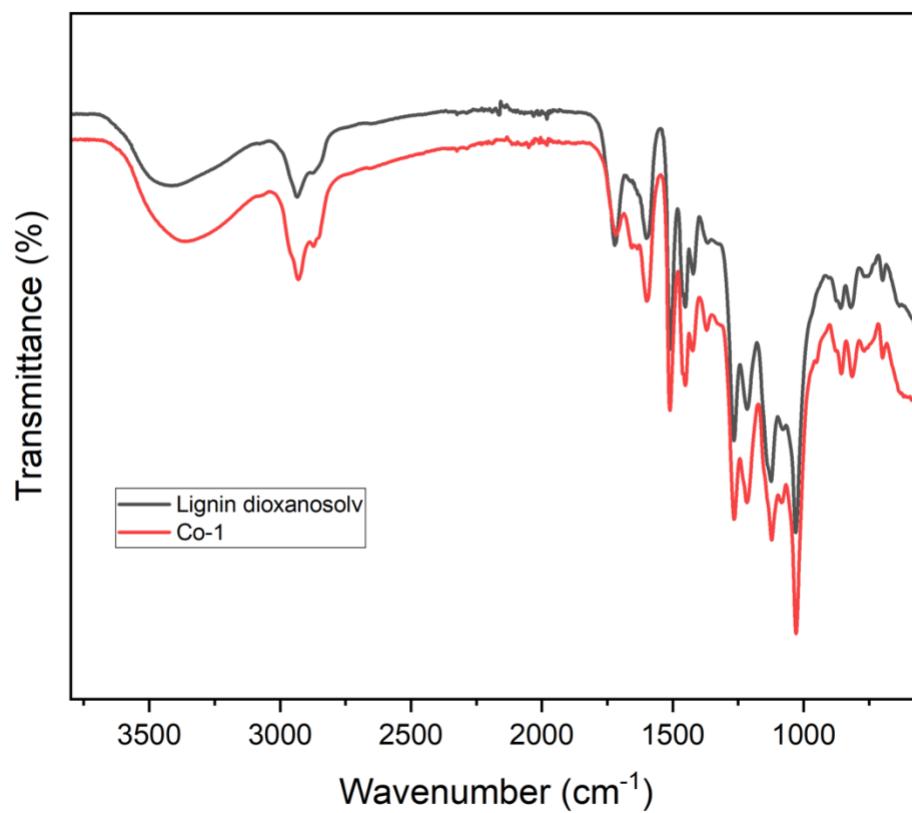


**Figure S44.** FTIR spectrum of dioxanosolv lignin hydrogenolysis with **Co-1**.

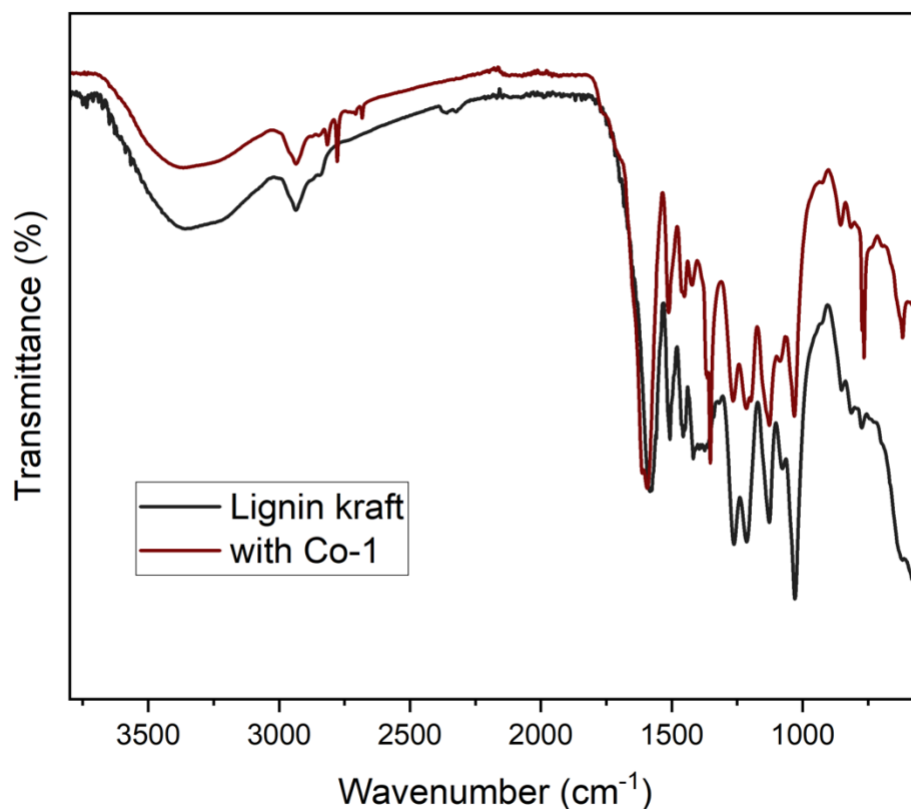


Figure S45. FTIR spectrum of kraft lignin hydrogenolysis with Co-1.

## 7. References

- 1 M. C. Biesinger, B. P. Payne, A. P. Grosvenor, L. W. M. Lau, A. R. Gerson and R. S. C. Smart, *Appl. Surf. Sci.*, 2011, **257**, 2717–2730.
- 2 J. Yang, H. Liu, W. N. Martens and R. L. Frost, *J. Phys. Chem. C*, 2010, **114**, 111–119C. S.
- 3 Lancefield, L. W. Teunissen, B. M. Weckhuysen and P. C. A. Bruijninx, *Green Chem.*, 2018, **20**, 3214–3221.
- 4 G. H. Major, N. Fairley, P. M. A. Sherwood, M. R. Linford, J. Terry, V. Fernandez and K. Artyushkova, *J. Vac. Sci. Technol. A*, 2020, **38**, 061203.
- 5 R. V. Jagadeesh, T. Stemmler, A.-E. Surkus, M. Bauer, M.-M. Pohl, J. Radnik, K. Junge, H. Junge, A. Brückner and M. Beller, *Nat. Protoc.*, 2015, **10**, 916–926.
- 6 J. M. Nichols, L. M. Bishop, R. G. Bergman and J. A. Ellman, *J. Am. Chem. Soc.*, 2010, **132**, 16725–16725.
- 7 M. V. Galkin, S. Sawadjoon, V. Rohde, M. Dawange and J. S. M. Samec, *ChemCatChem*, 2014, **6**, 179–184.
- 8 P. Aguilón-Rodríguez, O. Pérez-Reyes and C. Ortiz-Cervantes, *Results Chem.*, 2023, **5**, 100729.
- 9 T. H. Parsell, B. C. Owen, I. Klein, T. M. Jarrell, C. L. Marcum, L. J. Hauptert, L. M. Amundson, H. I. Kenttämä, F. Ribeiro, J. T. Miller and M. M. Abu-Omar, *Chem. Sci.*, 2013, **4**, 806–813.
- 10 Q. Wang, L.-P. Xiao, Y.-H. Lv, W.-Z. Yin, C.-J. Hou and R.-C. Sun, *ACS Catal.*, 2022, **12**, 11899–11909.
- 11 T. Li, B. Chen, M. Cao, X. Ouyang, X. Qiu and C. Li, *AIChE J.*, 2023, **69**, 1–12.
- 12 X. Liu, H. Li, L.-P. Xiao, R.-C. Sun and G. Song, *Green Chem.*, 2019, **21**, 1498–1504.
- 13 M. Chin, S. M. Suh, Z. Fang, E. L. Hegg and T. Diao, *ACS Catal.*, 2022, **12**, 2532–2539.
- 14 Z. Liu, H. Li, X. Gao, X. Guo, S. Wang, Y. Fang and G. Song, *Nat. Commun.*, 2022, **13**, 4716.